

10/4-15-97 JSD

# SANDIA REPORT

SAND97-8245 • UC-406  
Unlimited Release  
Printed March 1997

M97052496

## Modification of the Sandia National Laboratories/California Advanced Coordinate Measuring Machine for High Speed Scanning

J. M. Baldwin, R. D. Pilkey, R. M. Cassou, K. D. Summerhays, R. P. Henke

Prepared by  
Sandia National Laboratories  
Albuquerque, New Mexico 87185 and Livermore, California 94551  
for the United States Department of Energy  
under Contract DE-AC04-94AL85000

Approved for public release; distribution is unlimited.



# MASTER

HH

DISTRIBUTION OF THIS DOCUMENT IS UNLIMITED

Issued by Sandia National Laboratories, operated for the United States Department of Energy by Sandia Corporation.

**NOTICE:** This report was prepared as an account of work sponsored by an agency of the United States Government. Neither the United States Government nor any agency thereof, nor any of their employees, nor any of the contractors, subcontractors, or their employees, makes any warranty, express or implied, or assumes any legal liability or responsibility for the accuracy, completeness, or usefulness of any information, apparatus, product, or process disclosed, or represents that its use would not infringe privately owned rights. Reference herein to any specific commercial product, process, or service by trade name, trademark, manufacturer, or otherwise, does not necessarily constitute or imply its endorsement, recommendation, or favoring by the United States Government, any agency thereof or any of their contractors or subcontractors. The views and opinions expressed herein do not necessarily state or reflect those of the United States Government, any agency thereof, or any of their contractors or subcontractors.

This report has been reproduced from the best available copy.

Available to DOE and DOE contractors from:

Office of Scientific and Technical Information  
P.O. Box 62  
Oak Ridge TN 37831

Prices available from (615) 576-8401, FTS 626-8401.

Available to the public from:

National Technical Information Service  
U.S. Department of Commerce  
5285 Port Royal Rd.  
Springfield, VA 22161

## **DISCLAIMER**

**This report was prepared as an account of work sponsored by an agency of the United States Government. Neither the United States Government nor any agency thereof, nor any of their employees, make any warranty, express or implied, or assumes any legal liability or responsibility for the accuracy, completeness, or usefulness of any information, apparatus, product, or process disclosed, or represents that its use would not infringe privately owned rights. Reference herein to any specific commercial product, process, or service by trade name, trademark, manufacturer, or otherwise does not necessarily constitute or imply its endorsement, recommendation, or favoring by the United States Government or any agency thereof. The views and opinions of authors expressed herein do not necessarily state or reflect those of the United States Government or any agency thereof.**

**DISCLAIMER**

**Portions of this document may be illegible in electronic image products. Images are produced from the best available original document.**

SAND97-8245  
Unlimited Release  
Printed March 1997

# **MODIFICATION OF THE SANDIA NATIONAL LABORATORIES/CALIFORNIA ADVANCED COORDINATE MEASURING MACHINE FOR HIGH SPEED SCANNING**

Jon M. Baldwin, Robert D. Pilkey  
Integrated Manufacturing Systems  
Sandia National Laboratories/California

Ronald M. Cassou, Kim D. Summerhays  
University of San Francisco  
San Francisco, California

Richard P. Henke  
MicroVu  
Windsor, California

## **ABSTRACT**

The Moore M48V high accuracy coordinate measuring machine (CMM), while mechanically capable of exact measurement of physical artifacts, is not, in its original configuration, well suited for rapid gathering of high density dimensional information. This report describes hardware and software modifications to the original control and data acquisition system that allow relatively high speed scanning of cylindrical features. We also estimate the accuracy of the individual point data on artifacts measured with this system and provide detailed descriptions of the hardware and software apparatus as an aid to others who may wish to apply the system to cylindrical or other simple geometries.

## CONTENTS

	<u>Page</u>
I. Introduction .....	7
II. Data Acquisition System Modification .....	8
Description of the Original M48V Control and Data Acquisition System .....	8
Modifications to Data Acquisition and Control Electronics .....	9
III. Probing System Modifications .....	11
Probe System Calibration .....	11
IV. Artifact Fixturing and Location .....	14
Description of Cylinder Artifact .....	14
Fixture Description .....	14
Fixture Calibration .....	15
V. Error Budget Calculations .....	19
Thermally-induced Errors .....	19
Errors in $r$ .....	19
Errors due to spindle axis offset from feature axis .....	19
Error due to varying contact point of the probe tip .....	19
Error due to variation of effective probe offset from spindle axis .....	24
Positioning error of x- and y-axes .....	26
Uncertainty of indicator calibration .....	26
Error due to variation of the voltage divider ratio .....	26
Failure of the electronic indicator to act as a one-dimensional sensor .....	26
Uncertainty in the x- and y-axis reference locations .....	26
Uncertainty of the probe tip radius .....	27
Total error in $r$ .....	27
Errors in $\theta$ .....	27
Positioning error of the spindle axis .....	27
Uncertainty in the zero position of the spindle axis .....	27
Total error in $\theta$ .....	27
Errors in $z$ .....	28
Positioning error of the z-axis .....	28
Uncertainty in the z-axis reference location .....	28
Variation of artifact thickness .....	28
Total error in $z$ .....	28
Summary .....	28
VI. References .....	30
Appendix A: Data Acquisition Program .....	31
Appendix B: Typical Motion Control Programs .....	39
SCANMAIN .....	40
POSINCYL .....	42
SCANCYL .....	42
Appendix C: Machine Drawing of the Cylinder Artifact .....	44

## ILLUSTRATIONS

<u>No.</u>	<u>Page</u>
1. Schematic diagram of the original M48V data acquisition and control system . . . . .	8
2. Schematic diagram of the modified M48V data acquisition and control system . . . . .	9
3. Electronic indicator mounted in the c-axis quill of the M48V . . . . .	12
4. Internal cylindrical feature artifact . . . . .	14
5. Artifact-positioning fixture and calibration hardware . . . . .	15
6. Close-up view of artifact-positioning fixture . . . . .	16
7. Fixture z-reference calibration . . . . .	17
8. Error in r due to varying point of probe contact . . . . .	20
9. Error in r due to varying point of probe contact; detail showing probe tip geometry . . . . .	22
10. Scale of Figure 8 distorted to show geometry at the probe tip . . . . .	23
11. Error due to spindle axis offset; $r_{ball}=0$ . . . . .	24
12. Cylinder artifact; top view . . . . .	45
13. Cylinder artifact; bottom view . . . . .	46
14. Cylinder artifact; side view . . . . .	47
15. Cylinder artifact; section view . . . . .	47
16. Cylinder artifact; detail A . . . . .	48
17. Cylinder artifact; detail B . . . . .	49
18. Cylinder artifact; detail C . . . . .	50

## TABLE

<u>No.</u>	<u>Page</u>
C-1. List of full cylindrical features on the artifact . . . . .	51

# MODIFICATION OF THE SANDIA NATIONAL LABORATORIES/CALIFORNIA ADVANCED COORDINATE MEASURING MACHINE FOR HIGH SPEED SCANNING

## I. Introduction

The installation and capabilities of the Moore M48V coordinate measuring machine (CMM) at Sandia National Laboratories, Livermore, California have been described in an earlier report [1]. As normally configured, the M48V is equipped with a 3D analog probe head with 3 axis position sensing capability and can perform three-dimensional measurements of artifacts up to 1220 mm × 813 mm × 508 mm (48 in × 32 in × 20 in) in size with a typical volumetric uncertainty of 1.5 μm (60 μin) over the measuring volume. Complete performance specifications are given in the above-referenced report. A major limitation of the M48V CMM as originally installed is a low maximum data acquisition rate, about one point per 10 seconds. The original system is thus unsuited for the rapid acquisition of high density dimensional information. Additionally, the standard probing system has a relatively narrow linear dynamic range, ±0.050 mm (0.002 in), rendering impossible automated measurement of features with errors approaching that value.

Recent collaborative research, involving workers from Sandia National Laboratories, California, the University of San Francisco and Allied Signal/Federal Manufacturing & Technology Division, has been directed at investigating efficient and accurate methods for sample pattern selection and data analysis in point-sample methods of dimensional metrology [2-4]. Key to the success of that work has been the acquisition of high density ( $\approx 10^3$  to  $10^4$  points/feature) data on series of nominally identical machined metal artifacts.

While the M48V is ideally suited to this work from the point of view of accuracy and resolution, the achievable data rate was obviously a prohibitive factor. Additionally, the linear dynamic range of the standard probing system is readily exceeded by many machined surfaces. This report describes modifications to the M48V probing system and data acquisition electronics which relieve these limitations for simple (cylindrical, planar) feature geometries. Following sections of this report describe: a) modifications to the original sensing and data acquisition systems, b) software for CMM control and data acquisition, c) fixturing and datum establishment for artifacts with internal cylindrical features and d) error budget calculations. We also present detailed information on data gathering and motion control programs as well as on the design of the artifact.



## II. Data Acquisition System Modification

### Description of the Original M48V Control and Data Acquisition Systems

These systems are described more completely in the earlier report [1]. The following brief description is provided to set the context for the current modifications.

The original control and data acquisition systems are shown schematically in Figure 1. In normal operation, machine control instruction files are created in the Hewlett Packard 330 Series computer and transmitted over a serial connection to the Allen Bradley Series 8200 CNC controller, which drives analog servo amplifiers and, in turn, the machine x-, y-, z- and c-axis servo motors.

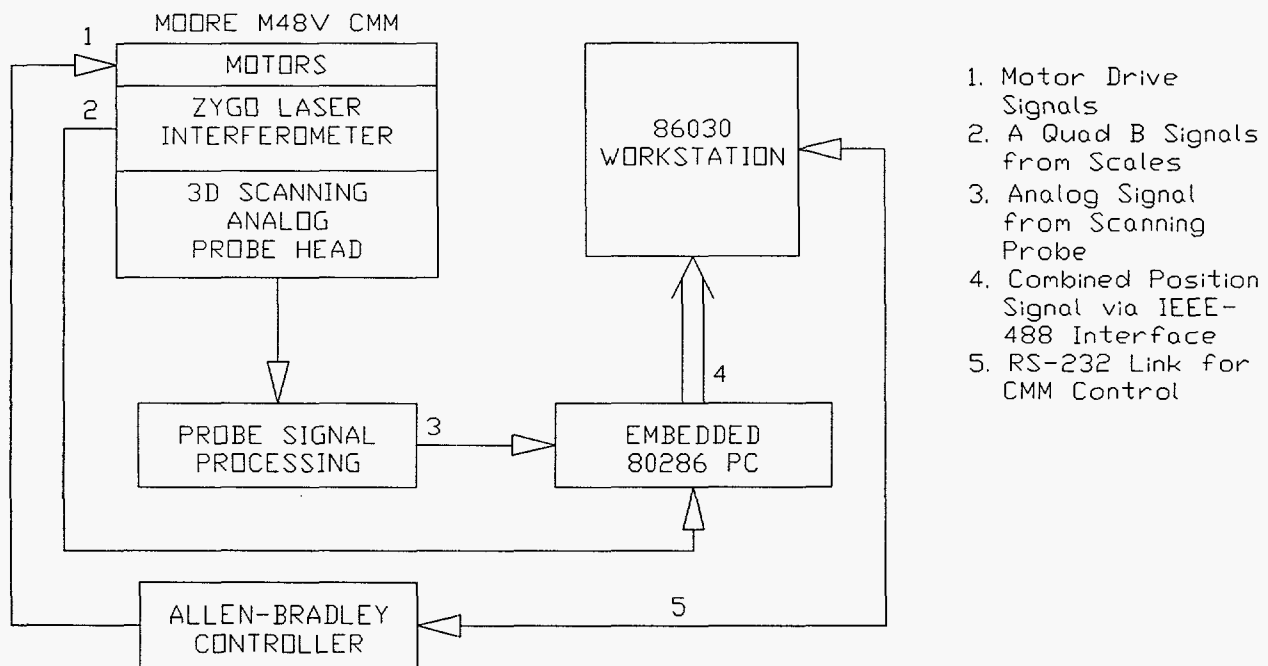


Figure 1. Schematic diagram of the original M48V data acquisition and control system.

Machine position information is provided, for the linear axes, by vacuum-path laser interferometers. Spindle axis angular information is provided by a rotary encoder with a resolution of  $10^{-5}$  revolution (0.0036 deg.). The axis position information is delivered, along with 3D probe deflection information, to an embedded processor which provides probe contact detection and position feedback to the Allen Bradley controller *via* a serial connection and part dimensional information to the Hewlett Packard computer through an IEEE-488 connection. It is a significant feature of the original design that absolute reference indications are not available for any of the machine axes. This limitation persists in the modified system and necessitates much of the calibration described in sections to follow.

Geometric data are processed and measurement reports generated with software executing on the Hewlett Packard computer. The maximum data rate capability of this system is approximately one point per 10 seconds, with the response characteristics of the Tridim probe, the maximum machine speed while probing and the processing power of the Hewlett Packard computer being the major limiting factors.

### Modifications to Data Acquisition and Control Electronics

The modified data acquisition and control system is shown in Figure 2. All of the major data rate limiting elements of the original system have been replaced.

The original motor drives were retained, along with the Allen Bradley controller. Motion control programs were written in the Allen Bradley control language [5], either by direct keypad entry at the Allen Bradley control panel or with a text editor running on the 80386-based computer, in which case they were subsequently uploaded to the controller over the serial link.

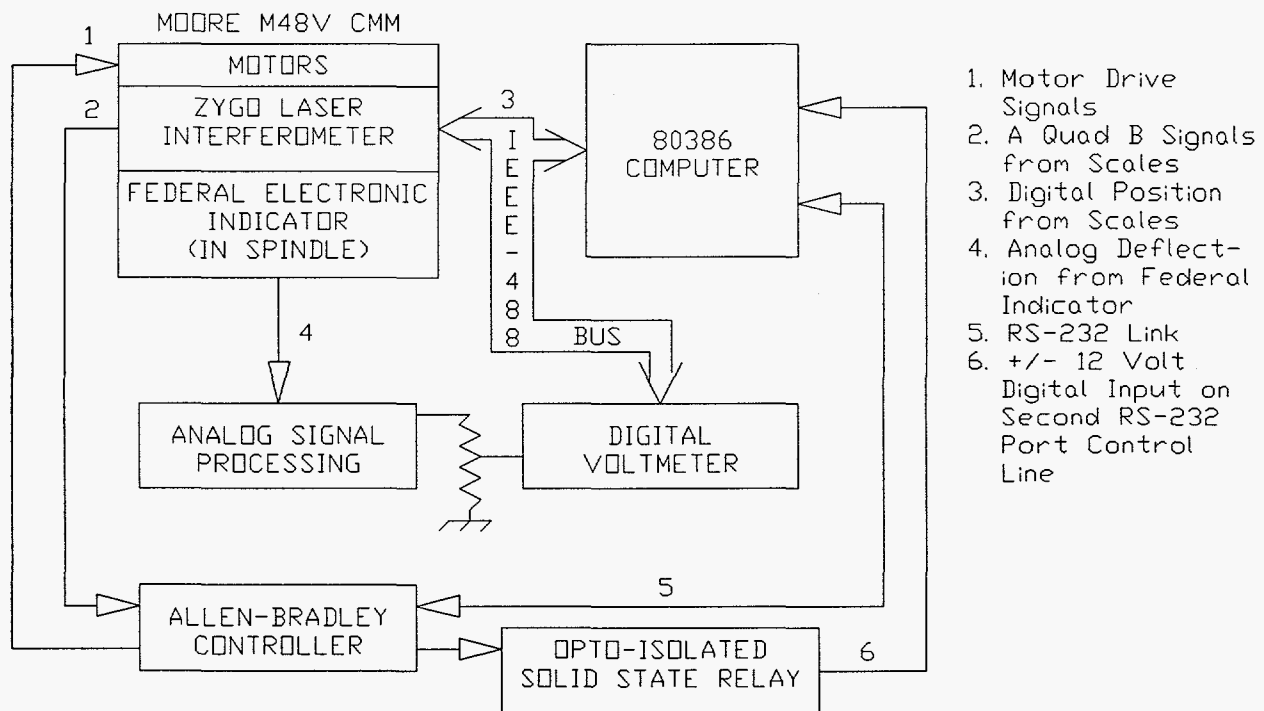


**Figure 2. Schematic diagram of the modified M48V data acquisition and control system.**

The original probing system was replaced by a Federal electronic indicator mounted in the rotary spindle. The analog output of the electronic indicator was divided by a thin film resistor divider to match the ranges available on the Hewlett Packard Model 3437A digital voltmeter. The voltage divider had a nominal total resistance of 20 K $\Omega$  and was calibrated with a precision voltage source and a digital voltmeter having a resolution of 1:10<sup>7</sup> of full scale. Thermally-induced resistance fluctuations due to varying power dissipation were a matter for concern. Readings were taken at

applied voltages of one and five volts (nominally, currents of 0.05 and 0.25 ma), waiting in each case for the voltage reading at the divider tap to stabilize. Divider ratios of  $0.400276 \pm 0.000001$  and  $0.400273 \pm 0.000002$ , respectively, were observed. The uncertainty in the divider ratio is thus seen to be on the order of  $2:10^5$ , inclusive of thermal effects. The voltmeter digital output, corresponding to the radial deflection of the indicator, was transmitted over the IEEE-488 bus to the data collection computer.

Axis position data for the linear axes was transmitted from the laser interferometer to the data collection computer over the same IEEE-488 bus. In order to maximize data throughput the x- and y-axis positions were read only once per commanded z-axis move and assumed to be constant throughout the move while the c-axis position was assumed to be equal to the commanded position. These measures are not believed to significantly affect the accuracy of the results in view of the observed accuracy of the CMM [1] and the small following errors consistently observed ( $1-2 \mu\text{in}$  for the linear axes and  $1-2 \times 10^{-5}$  revolution for the c-axis). Scanning during data collection was solely along the z-axis. Under these conditions the maximum data acquisition rate was about 80 (r,  $\theta$ ) pairs/second. Data synchronization with the z-axis scan was achieved by using coolant on/off commands in the motion control program to toggle the solid state relay which, in turn, applied a  $\pm 12$  v signal to one of the control lines of a second serial port.

Typical CMM motion control and data acquisition programs are presented in Appendix B of this report.

### III. Probing System Modifications

The standard probing system used with the M48V is a Movomatic Tridim™ 3-directional analog sensor with a display resolution in each axis of about 0.025  $\mu\text{m}$  (1  $\mu\text{in}$ ). While capable of more than adequate accuracy for the present work, the mechanical response time of this probe and the electrical response of its associated data processing electronics constitute a major limiting element for the rate of data acquisition.

The simple shapes (planar, cylindrical) of interest in the present work, together with the CMM's rotating spindle (not normally used in conjunction with the Tridim probe) permit substitution of a single-axis electronic indicator. The indicator and mounting are shown in Figure 3. The indicator used in this work was a Federal Model A-D-4331 maximum reciprocal sensitivity of 10  $\mu\text{in/v}$ . In this work, it was used at a sensitivity of 200  $\mu\text{in/v}$  giving a linear dynamic range of  $\pm 0.001$  in. While not capable of the dimensional performance of the standard probing system, this will be shown to be more than adequate for the present study.

A separate mechanical setup of the electronic indicator was required for each nominal hole size. The offset of the indicator, relative to the spindle axis of rotation, was adjusted to give an approximately zero indicator output while sweeping a ring gage of the same size as the nominal hole with the spindle coaxial to the ring gage. Generally then, all holes of a given nominal size were scanned in the same measurement run.

#### Probe System Calibration

It was necessary to calibrate four aspects of the modified probing system.

First, the spindle axis position of zero rotation must be coincident with the direction of one of the Cartesian machine axes. This was accomplished by rotating the spindle either manually or by move commands entered from the controller console with the indicator bearing against a flat surface (gage block) mounted parallel to one of the Cartesian planes and with the indicator analog meter at maximum sensitivity, until maximum deflection was observed. The spindle axis count was zeroed at that point.

Second, it was necessary to know the linear deflection sensitivity of the indicator. This was determined by moving the indicator through its full range against the same flat surface as used to determine the c-axis zero position and observing the digital voltmeter signal as a function of linear axis position. The laser interferometer indication was taken to be accurate in this step. The least squares computed slope of output voltage vs. position typically had a relative standard deviation of 1:1000 ( $\pm 2 \times 10^{-7}$  in/V).

Third, the radius of the spherical probe tip was measured with a laser micrometer to an estimated uncertainty of  $\pm 15$   $\mu\text{in}$ .

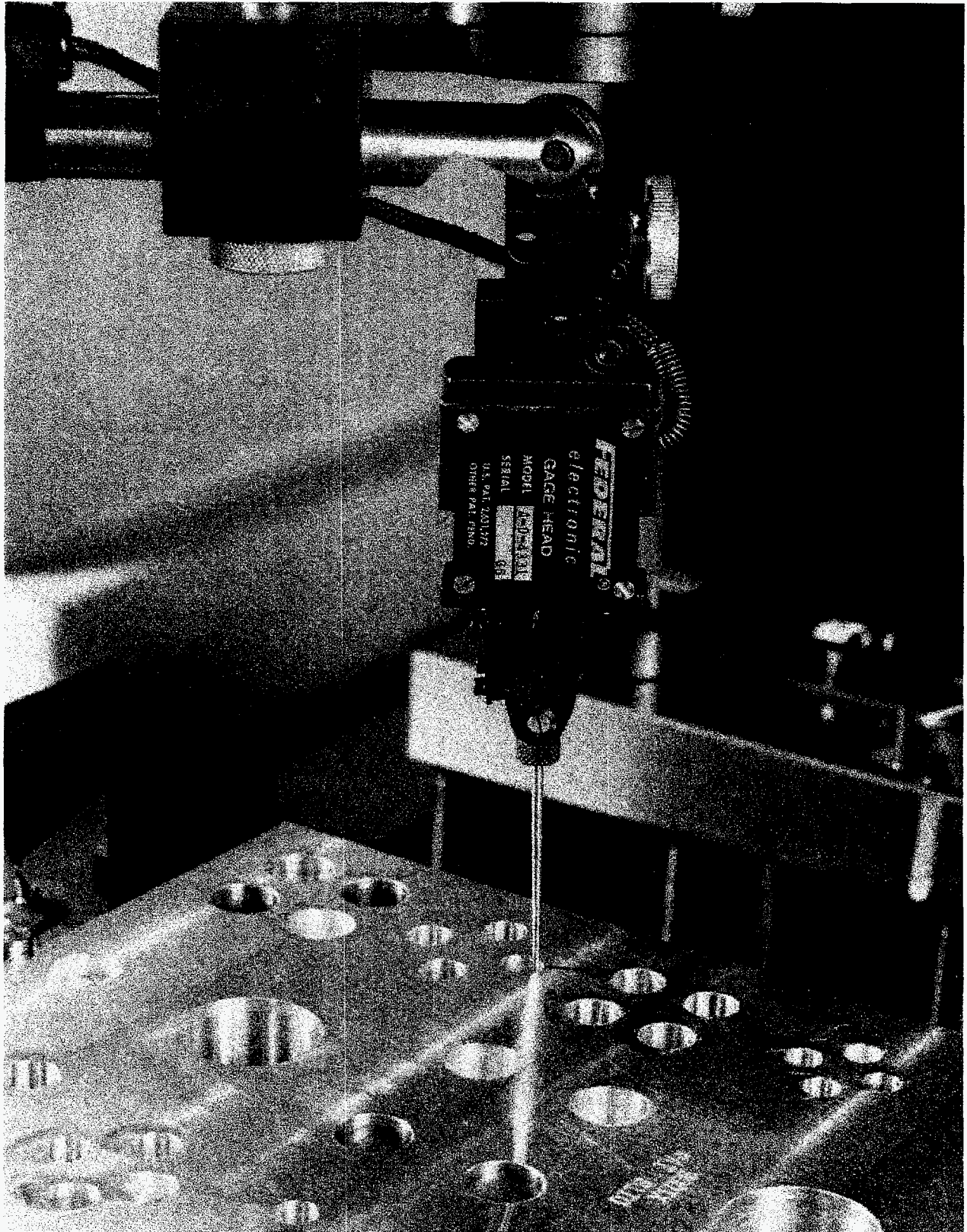


Figure 3. Electronic indicator mounted in the c-axis quill of the M48V.

Finally, it was necessary to know the indicator sweep radius for an output of 0 V with the indicator suitably set for the nominal hole size of the current experiment. This was determined by sweeping a ring gage of a size equal to the nominal hole size. Generally, the ring gage diameter was known to  $\pm 0.5 \mu\text{m}$ . The spindle was first centered on the ring gage by looking for the point of constant deflection while manually sweeping the ring. Eight voltage readings were then taken at equal angular intervals on the gage and a least squares circle fitted to the data, thereby providing an estimate of the desired quantity. These measurements were taken with the indicator analog meter set for  $\pm 0.001$  in full scale, no voltage divider and reading the voltage with an Hewlett Packard 3455A high resolution voltmeter.

The variation in indicator reading as the ring gage is swept can be approximated as

$$\Delta r = r_{\text{RING}} - r_{\text{FED}} + A \cos \theta + B \sin \theta$$

where  $r_{\text{RING}}$  is the radius of the ring gage,  $r_{\text{FED}}$  is the sweep radius of the electronic indicator,  $\theta$  is the angle of rotation of the spindle and  $r_{\text{FED}}$ , A and B are parameters to be determined. If

$$D = r_{\text{RING}} - r_{\text{FED}}$$

then

$$\Delta r = D + A \cos \theta + B \sin \theta$$

which we can fit, in the least squares sense, to the observed data to get an estimate of D and thereby of  $r_{\text{FED}}$ . The standard deviation of D by this method was typically  $2 \mu\text{in}$  giving a total uncertainty in  $r_{\text{FED}}$  of about  $\pm 2.5 \mu\text{in}$ .

## IV. Artifact Fixturing and Location

### Description of Cylinder Artifact

The initial subject of this work was a series of 30 nominally identical artifacts intended to provide machining process characteristics data on internal cylindrical features. The artifact design is shown schematically in Figure 4. It contains 50 full internal cylindrical features, through, blind and counterbored, of various sizes and depths, and produced by a variety of machining techniques. All holes were started with a center drill operation, followed by drilling to near nominal size. Some of the holes were further finished by reaming, boring/reaming, plunge end milling, or peripheral milling. Full specifications of the artifact are given in Appendix C.

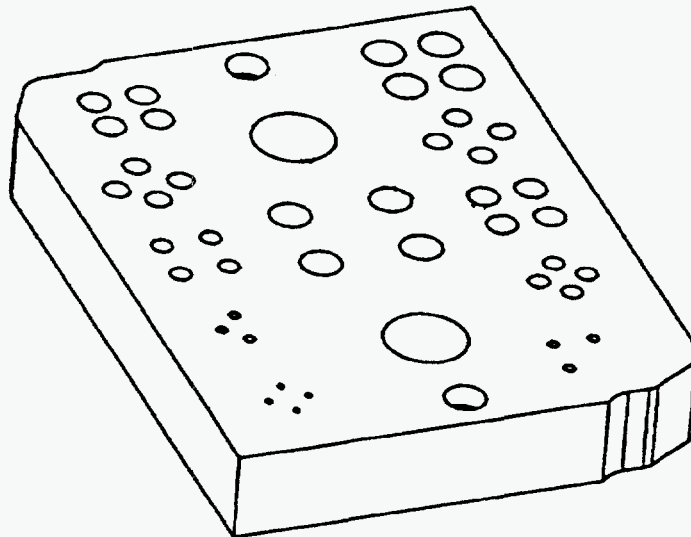
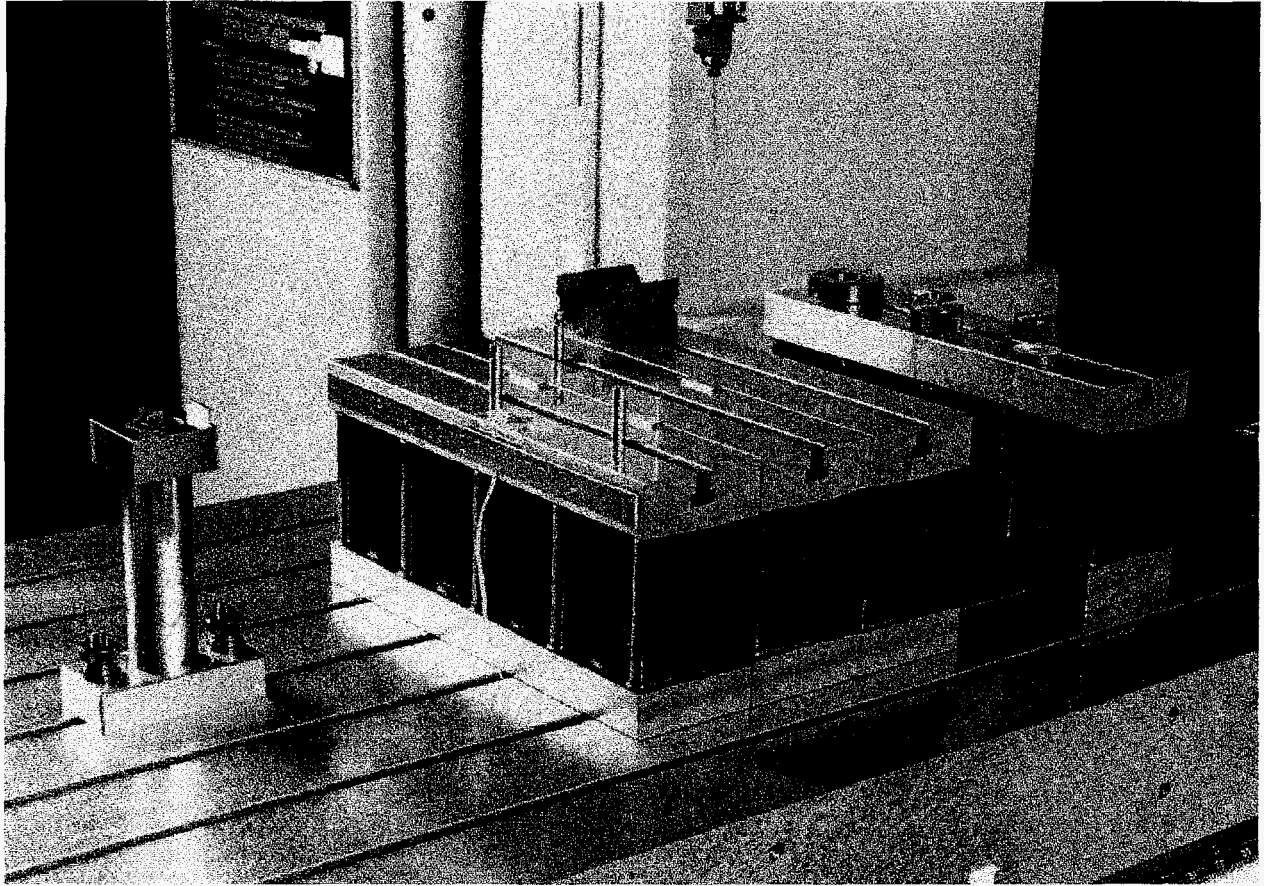


Figure 4. Internal cylindrical feature artifact.

### Fixture Description

The artifact fixturing arrangement is shown in Figures 5 and 6. The bottom surface of each artifact was mechanically deburred against a granite surface plate prior to measurement. That surface was located against 3-0.0100 in gage blocks which were, in turn, fixed with epoxy cement to a set of 6 in precision parallels placed on the measuring machine table. Part alignment and x-y



**Figure 5. Artifact-positioning fixture and calibration hardware.**

location were provided by 3 cylindrical pins fixed in the t-slots of the parallels. Two of these pins were mechanically aligned with the measuring machine y-axis.

### **Fixture Calibration**

Given the lack of an absolute machine reference, it was necessary to express the motion control program relative to a fixed location on the artifact and then to accurately establish the location of the artifact relative to the current machine scale zero points.

An x-y location in the machine's coordinate system was established by assuming the first artifact (serial #002) to be typical of the entire production run. The lower 0.375 in dia reference hole was located in the machine's coordinate system by placing the artifact in the fixture, manually indicating its location with the electronic indicator and noting the x and y scale readings. These readings were recorded and entered as parameters of the motion control program (see **Appendix B: Typical Motion Control Programs**). Even though the pair of reference holes were specified as a machining datum they were not of particularly better form (roundness  $\approx 0.0005$  in) than the other cylindrical features and therefore constitute a significant source of error in measured feature locations.



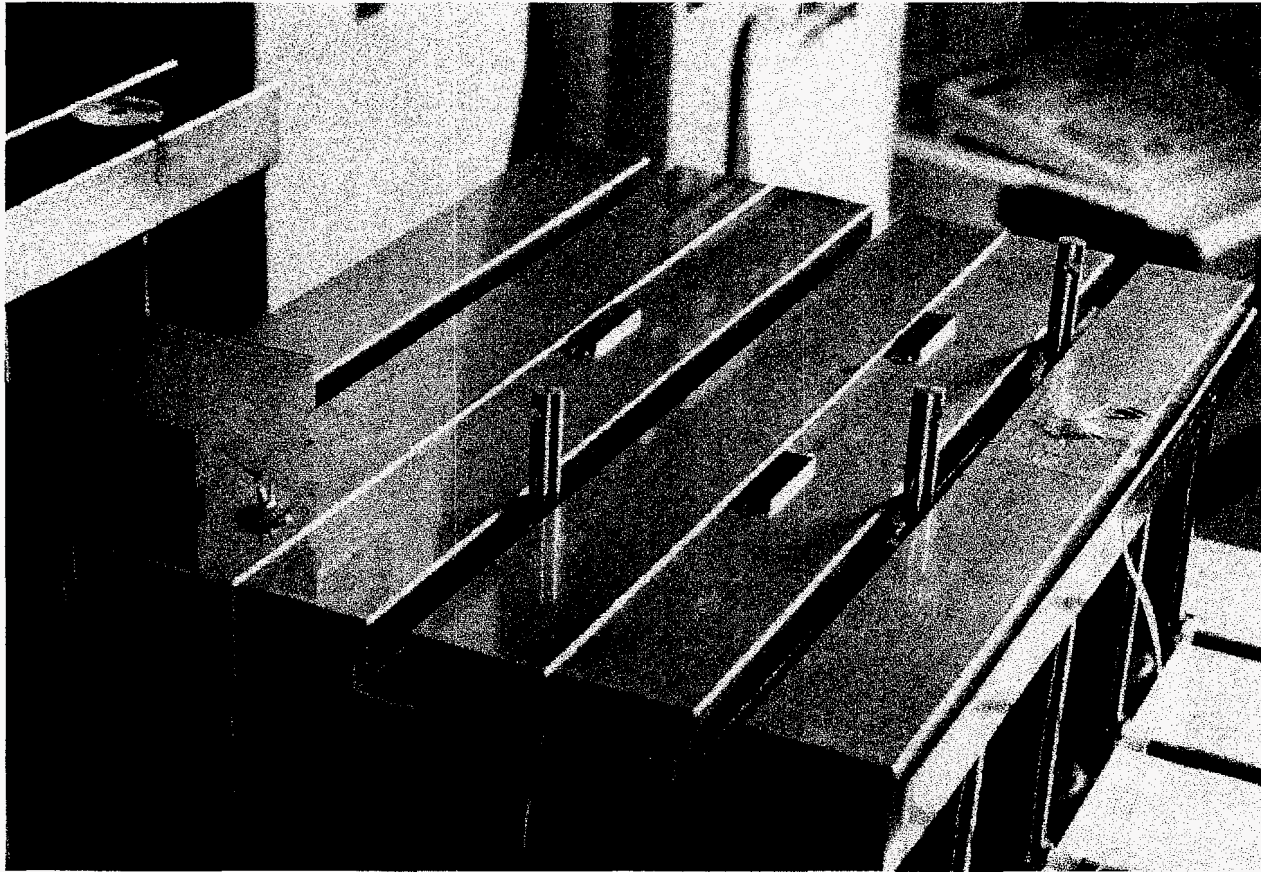


**Figure 6. Close-up view of artifact-positioning fixture.**

Note that this operation must precede the mechanical adjustment and calibration of the probe described under **Probe System Calibration**.

A z-axis reference was computed as the machine coordinate system location of the top surface of artifact #2 when in position in the fixture. A V-block with an included angle of approximately  $90^\circ$  was measured on a utility (0.0001 in resolution) coordinate measuring machine and found to have an included angle of  $2\theta = 89.950 \pm 0.001^\circ$  and a distance from the bottom of the V-groove to the base of  $d = 0.4404 \pm 0.0002$  in (standard deviation). The block was then aligned with the machine x-axis and fixed to the top of the parallel. Refer to Figure 7. The spindle was rotated so that the indicator sensitive direction was parallel to the machine y-axis, the machine y location adjusted to null the indicator against one face of the V and the y- and z-axis positions noted. The spindle was then rotated  $180^\circ$  and the process repeated at the other face and the same xz location. Then if the probe tip radius is  $r_{ball}$ , the difference of the y-axis coordinates of the probe tip center locations is  $\Delta y$ , the half angle of the V-block is  $\theta$ , the remaining quantities are as defined in Figure 7 and we take the symmetry plane of the V to be perpendicular to the base we can calculate the total width of the V at the center of the probe tip:

$$l_1 = r_{\text{ball}} / \cos \theta_1$$

$$l_2 = r_{\text{ball}} / \cos \theta_2$$

$$l_1 = l_2 = r_{\text{ball}} / \cos \theta$$

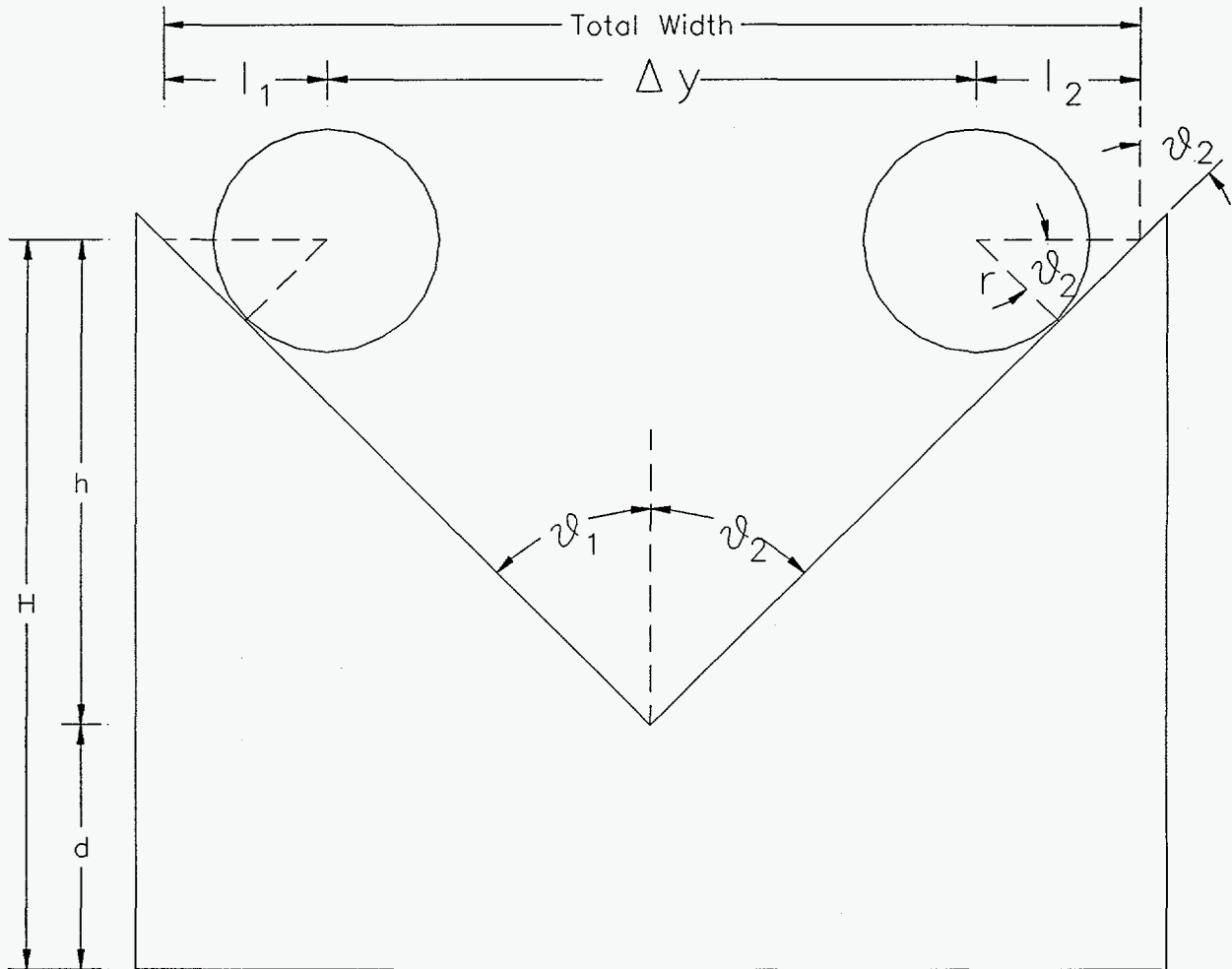


Figure 7. Fixture z-reference calibration.

Then if  $\Delta y_{AB}$  is the indicated difference in y-axis position at the two null locations and  $r_{\text{FED}}$  is the sweep radius of the indicator as determined earlier

$$\Delta y = \Delta y_{AB} + 2(r_{\text{FED}} - r_{\text{ball}})$$

and

$$\begin{aligned}\text{total width} &= W_T = l_1 + l_2 + \Delta y \\ W_T &= 2r/\cos\theta + \Delta y_{AB} + 2(r_{FED} - r_{ball})\end{aligned}$$

Again invoking the assumption that  $\theta_1 = \theta_2 = \theta$  we have

$$W_T = 2h \tan\theta$$

By combining these last two expressions and rearranging,

$$h = \frac{1}{(2 \tan\theta)} \left[ 2r \left( \frac{1}{(\cos\theta)} - 1 \right) + \Delta y_{AB} + 2r_{FED} \right]$$

Adding the measured distance,  $d$ , from the bottom of the V to the bottom of the block, we get for the  $z$  distance from the probe tip center to the bottom of the V-block:

$$H = \frac{1}{(2 \tan\theta)} \left[ 2r_{ball} \left( \frac{1}{\cos\theta} - 1 \right) + \Delta Y_{AB} + 2r_{FED} \right] + d$$

and the machine coordinate system  $z$  location of the top of an artifact is

$$z_{ref} = z_{ball} - H + h_{gage} + z_{part}$$

where  $z_{ball}$  is the machine coordinate  $z$  position of the center of the ball when probing the V-block,  $h_{gage}$  is the height of the supporting gage blocks and  $z_{part}$  is the measured height of the artifact.

## V. Error Budget Calculations

It is of interest to have an estimate of the error in each of the three coordinates defining the probe point of contact with the artifact. In general, there are several sources of error in each coordinate. In most instances, we are able to estimate the worst case error. Errors that can reasonably be judged out of hand to be insignificant will not be treated. All error estimates are thought to represent the total worst-case error bandwidth. The total error in each coordinate is obtained by combining as the rms sum all the significant error sources.

It is, furthermore, interesting to consider the effect of errors in the individual point coordinates on the accuracy of derived parameters. Ideally, the individual point errors could be propagated through subsequent fitting algorithms to yield estimates of the resultant errors in the defining parameters of the fitted shapes. Such consideration is beyond the scope of this report. We will limit our consideration to enumeration of the most influential error source(s) for each defining parameter of the fitted cylinder. Extension to other simple geometries is straightforward.

### Thermally-induced errors

Thermal control of the measuring machine environment was described in the earlier report [1]. Room temperature control of  $\pm 0.12$  °C is generally achieved. The measured artifacts are fabricated from aluminum and are the system component most strongly influenced by temperature. Artifact temperature was monitored and generally was constant to better than  $\pm 0.1$  °C. Over the approximately 10 inch largest dimension of the artifact this would be represented by a length change of about 12  $\mu$ m or on the order of 1/10 or less of that value over a single feature.

### Errors in r

#### Errors due to spindle axis offset from feature axis

##### Error due to varying contact point of the probe tip

This is the error caused by contacting the (possibly perfectly circular) feature surface with a probe of finite radius when the spindle axis is not coincident with the feature center. Refer to Figures 8 -10. C is the center of the measured feature and C' is the center of rotation of the spindle. r is the true feature radius, r' the apparent feature radius and  $\Delta r$  the distance between C and C', with the angles  $\alpha$  and  $\psi$  as shown in the figures. We first need to find  $\psi(\alpha, r, \Delta r)$ :

$$(\Delta r)^2 = r^2 + r'^2 - 2rr' \cos \psi$$

and

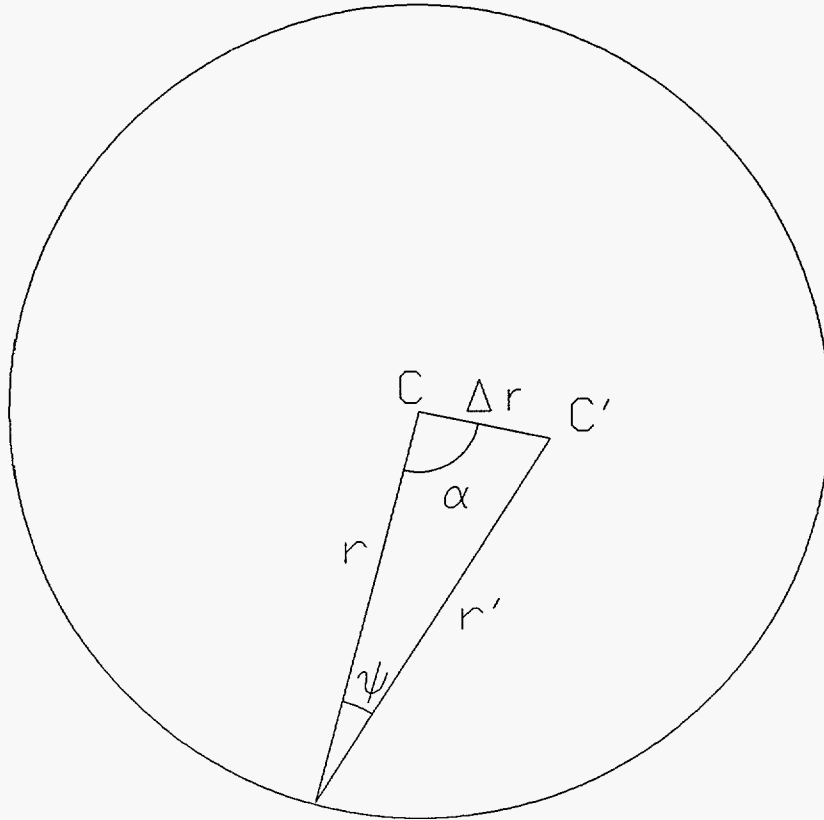


Figure 8. Error in  $r$  due varying point of probe contact.

$$r'^2 = r^2 + (\Delta r)^2 - 2r\Delta r \cos \alpha$$

Combining these expressions,

$$(\Delta r)^2 = [2r^2 + (\Delta r)^2 - 2r\Delta r \cos \alpha] - 2r[r^2 + (\Delta r)^2 - 2r\Delta r \cos \alpha]^{1/2} \cos \psi$$

and rearranging,

$$\cos \psi = \left[ 1 - \frac{\Delta r}{r} \cos \alpha \right] \left[ 1 + \left( \frac{\Delta r}{r} \right)^2 - 2 \left( \frac{\Delta r}{r} \right) \cos \alpha \right]^{-1/2}$$

When  $\psi$  is a maximum we will have the maximum error due to not always contacting the same point on the probe tip. For maximum  $\psi$ ,  $\cos \psi$  will be a minimum so at that point we will have

$$\frac{d(\cos \psi)}{d\alpha} = 0$$

or

$$\left(-\frac{\Delta r}{r}\right)(-\sin \alpha) \left[1 + \left(\frac{\Delta r}{r}\right)^2 - \frac{2\Delta r}{r} \cos \alpha\right]^{-1/2} + \left[1 - \frac{\Delta r}{r} \cos \alpha\right] \left(\frac{1}{2}\right) \left[1 + \left(\frac{\Delta r}{r}\right)^2 - \left(\frac{2\Delta r}{r}\right) \cos \alpha\right]^{-3/2} \left(-\frac{2\Delta r}{r}\right)(-\sin \alpha) = 0$$

and by rearranging and simplifying we have the maximum error at

$$\alpha = \cos^{-1}\left(\frac{\Delta r}{r}\right)$$

Substituting for  $\alpha$  in the earlier expression for  $\cos \psi$  we get for the value of  $\cos \psi$  corresponding to the maximum error

$$\cos \psi = \left[1 - \frac{\Delta r}{r} \frac{\Delta r}{r}\right] \left[1 + \left(\frac{\Delta r}{r}\right)^2 - 2 \frac{\Delta r}{r} \frac{\Delta r}{r}\right]^{-1/2}$$

or

$$\cos \psi = \left[1 - \left(\frac{\Delta r}{r}\right)^2\right]^{1/2}$$

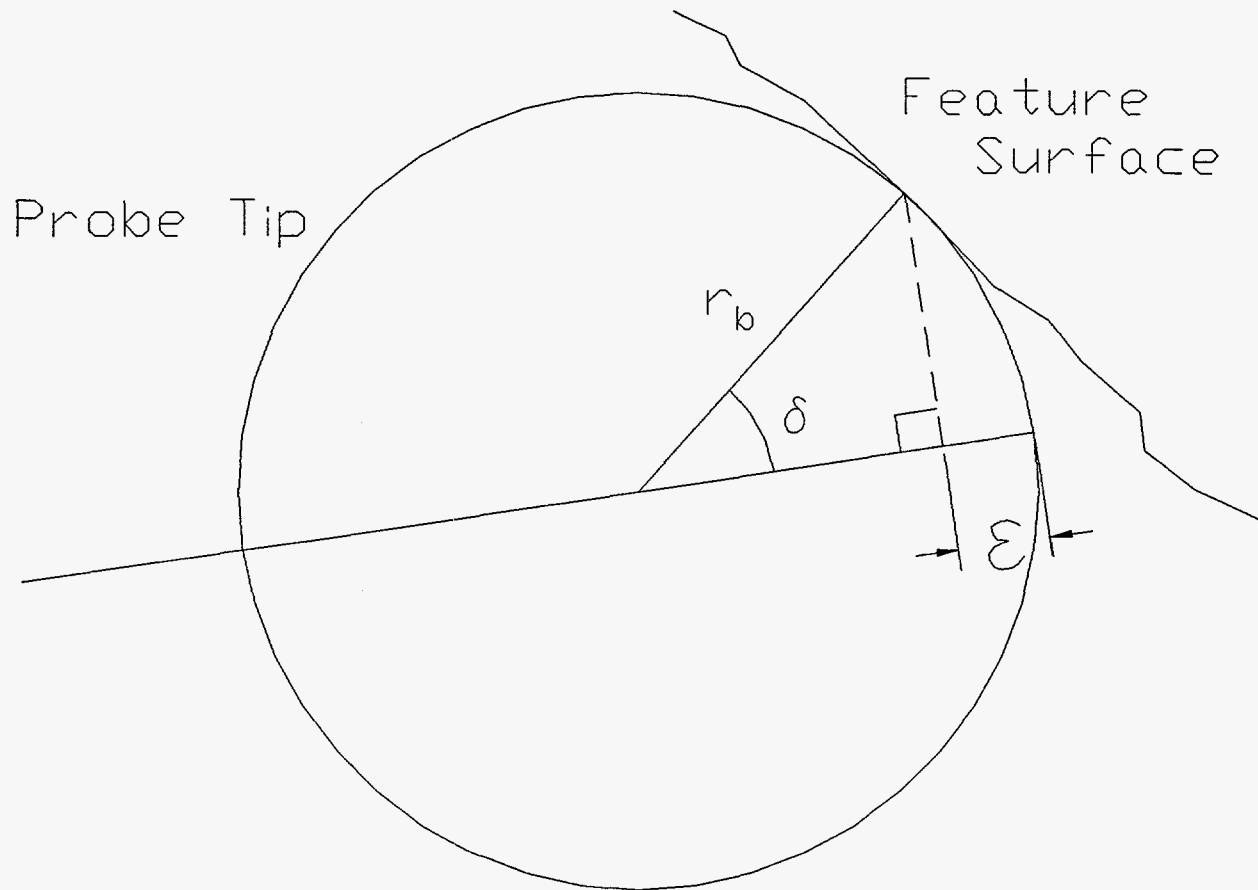


**Figure 9. Error in  $r$  due to varying probe contact; detail showing probe tip geometry.**

Referring to Figure 9 we see that the error  $\epsilon$  in  $r'$  due to the probe center not lying on the normal to the measured surface is given by

$$r_{\text{ball}} \cos \delta = r_{\text{ball}} - \epsilon$$

or

$$\epsilon = r_{\text{ball}}(1 - \cos \delta)$$

where  $r_{\text{ball}}$  is the radius of the measuring probe and  $\delta$  is the angle between the radius to the contact point and  $r'$ .

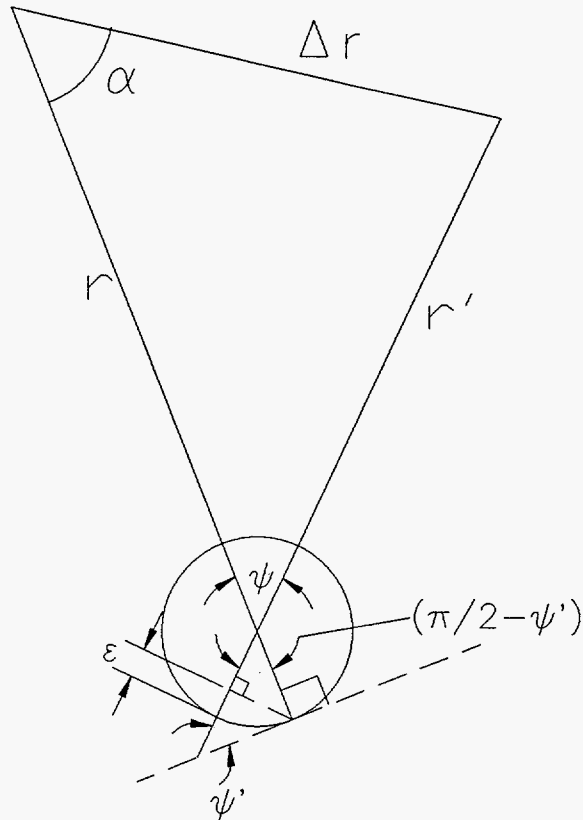


**Figure 10. Scale of Figure 8 distorted to show geometry at the probe tip.**

Then it is easily seen from Figure 10, an exaggerated version of Figure 8, that  $\delta = \psi$  and therefore

$$\epsilon = r_{\text{ball}}(1 - \cos \psi)$$

and substituting the value of  $\cos \psi$  corresponding to the maximum error

$$\epsilon_{\text{max}} = r_{\text{ball}} \left\{ 1 - \left[ 1 - \left( \frac{\Delta r}{r} \right)^2 \right]^{\frac{1}{2}} \right\}$$



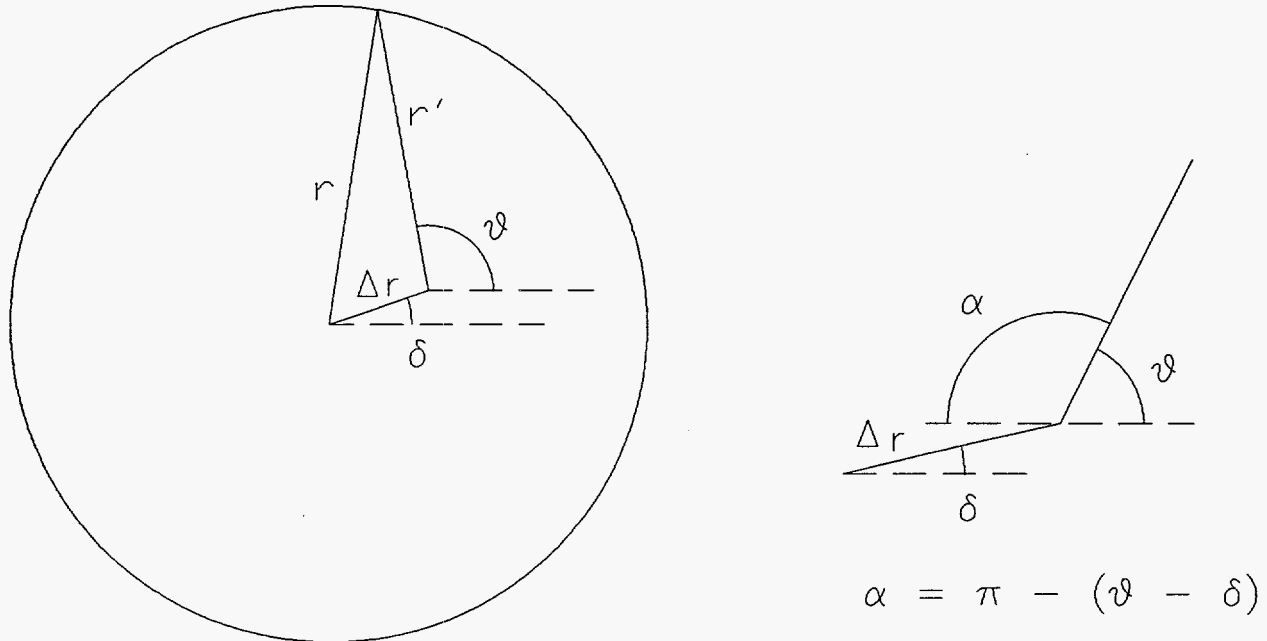


**Figure 11. Error due to spindle axis offset,  $r_{ball}=0$ .**

Note that this error always has the effect of reducing the apparent radius  $r'$ . The part-to-part variability from nominal of hole locations was about  $3.3 \times 10^{-4}$  in (standard deviation), independent of hole size and manufacturing technique. Substituting this value for  $\Delta r$  gives a worst case (95% C.I.) estimate for  $\epsilon_{max}$  of 1.6  $\mu\text{in}$ .

Error due to variation of effective probe offset from spindle axis

Refer to Figure 11. C is the center of the measured feature and C' is the center of rotation of the spindle.  $r$  is the true feature radius,  $r'$  the apparent feature radius and  $\Delta r$  the distance between C and C', with the angles  $\theta$  and  $\delta$  as shown in the Figure.  $\theta$  is the indicated angle of spindle rotation; angles are referenced to the  $0^\circ$  spindle axis location. Then

$$r^2 = (r')^2 + (\Delta r)^2 - 2r'\Delta r \cos \alpha$$

and with  $\alpha = \pi - (\theta - \delta) = -\cos(\theta - \delta)$

$$r = r' \left[ 1 + \left( \frac{\Delta r}{r'} \right)^2 + 2 \frac{\Delta r}{r'} \cos(\theta - \delta) \right]^{\frac{1}{2}}$$

Then expanding as a power series and discarding terms greater than second order

$$r \approx r' \left[ 1 + \frac{1}{2} \left( \frac{\Delta r}{r'} \right)^2 + \frac{\Delta r}{r'} \cos(\theta - \delta) - \frac{1}{2} \left( \frac{\Delta r}{r'} \right)^2 \cos^2(\theta - \delta) \right]$$

Since  $\cos(\theta - \delta) = \cos \theta \cos \delta + \sin \theta \sin \delta$  and letting

$$A = \Delta r \cos \delta$$

$$B = \Delta r \sin \delta$$

be the projected x- and y-components of  $\Delta r$  in the spindle coordinate system we can rewrite this as

$$r = r' + A \cos \theta + B \sin \theta + \frac{1}{2} r' \left( \frac{\Delta r}{r'} \right)^2 \sin^2(\theta - \delta)$$

or rearranging,

$$r' \approx r - A \cos \theta - B \sin \theta - \frac{1}{2} r' \left( \frac{\Delta r}{r'} \right)^2 \sin^2(\theta - \delta)$$

and the error due to neglecting second order terms, i.e. to fitting

$$r' = r - A \cos \theta - B \sin \theta$$

is

$$\epsilon^{\circ} = -\frac{1}{2} r' \left( \frac{\Delta r}{r'} \right)^2 \sin^2(\theta - \delta)$$

and since the maximum error occurs at  $\theta - \delta = \pi/2$  and since  $r' \approx r$

$$\epsilon_{\max}^{\circ} = -\frac{\Delta r^2}{2r}$$

Note that while this error may be significant in artifact measurement, it will become small in probe offset calibration since the spindle and ring gage centers were adjusted to be coincident to the order of  $10^{-5}$  in during ring gage calibration. Using the same range of values for  $\Delta r$  as previously we get for  $\epsilon_{\max}^{\circ}$  values (95% C.I.) of about 3  $\mu\text{in}$  for the 0.125 in diameter holes to much less than 1  $\mu\text{in}$  for 1 in diameter.

### **Positioning error of x- and y-axes**

The positioning error is less than 10  $\mu\text{in}$  in each axis [1] leading to a worst-case radial error  $\Delta r_{\text{pos}} \approx 14 \mu\text{in}$ .

### **Uncertainty of indicator calibration**

The uncertainty of the indicator calibration, as standard deviation of the least-squares slope was typically 1:1000 or less equating, for a full range deflection of  $\pm 0.001$  in, to a 95% C.I. band for  $\Delta r_{\text{ind}}$  of about 8  $\mu\text{in}$ . See **Probe System Calibration**.

### **Error due to variation of the voltage divider ratio**

The uncertainty in the divider ratio was earlier seen to be about  $2:10^5$ . In the worst case of a full scale indicator deflection (0.001 in) this results in an uncertainty in the radius indication of  $\Delta r_{\text{vd}} \approx 0.2 \mu\text{in}$ .

### **Failure of the electronic indicator to behave as a one-dimensional sensor**

Although the electronic indicator is designed to respond only to deflection normal to its pivot axis, deflection orthogonal to the sensitive direction is known to produce an output signal which will be observed as an error in  $r$ . The maximum error from this source is on the order of  $\Delta r_{2D} \approx 10 \mu\text{in}$  [6]. This estimate was borne out by the observed difference in indicated deflections at the same angle on ring gages, approached from opposite directions. In actual use, the error from this source was probably even less since the angular direction of approach was the same for all measurements.

### **Uncertainty in the x- and y-axis reference locations**

Reference location error in x and y must be considered in that the machine motion control program is expressed in machine coordinates, referred to the index hole (hole #1) of artifact serial #02. The location of this hole was determined by sweeping it with the electronic indicator and

adjusting the machine position to give a symmetrical indicator deflection. Error in the reference location will be reflected as a component of the machine quill axis to feature axis offset.

There are two components to reference location error: positioning repeatability of the artifact in the fixture and repeatability in determining the center of the index hole. The former is estimated to be on the order of 40  $\mu\text{in}$ . The latter is governed primarily by the form error of the index hole, which was on the order of 0.0005 in, limiting the repeatability of the location to about 20  $\mu\text{in}$ . Combining these components as the rms sum gives a total estimated error  $\Delta r_{\text{ref}}$  of 45  $\mu\text{in}$ .

### Uncertainty of the probe tip radius

The probe tip radius was measured with a laser micrometer to an estimated total uncertainty,  $\Delta r_{\text{ball}}$  of  $\pm 15 \mu\text{in}$ .

### Total error in r

For the smaller holes, the  $\epsilon^{\circ}_{\text{max}}$  term clearly dominates while for larger holes many terms contribute significantly. Combining the various components of uncertainty in r, as the rms sum, we have, in general:

$$\Delta r_{\text{total}} = (\Delta r_{\text{therm}}^2 + \epsilon_{\text{max}}^2 + \epsilon_{\text{max}}^0{}^2 + \Delta r_{\text{pos}}^2 + \Delta r_{\text{ind}}^2 + \Delta r_{\text{vd}}^2 + \Delta r_{\text{2D}}^2 + \Delta r_{\text{ref}}^2 + \Delta r_{\text{BALL}}^2)^{1/2}$$

Substituting the appropriate worst case values we get a value of  $\Delta r_{\text{total}} \approx 50 \mu\text{in}$ .

## Errors in $\theta$

### Positioning error of the spindle axis

The uncertainty in  $\theta$  due to positioning error of the spindle axis,  $\Delta \theta_{\text{pos}}$ , is on the order of 0.2 minutes of arc [1].

### Uncertainty in the zero position of the spindle axis

The minimum rotation of the spindle to produce an observable change of the indicator output, when the indicator was rotated against the gage block, was typically  $\Delta \theta_{\text{ref}} \approx 25$  minutes of arc. See **Probe System Calibration**.

### Total error in $\theta$

The uncertainty in the spindle axis zero, or reference, location dominates giving  $\Delta \theta_{\text{total}} \approx 25$  minutes.

## Errors in z

### Positioning error of the z-axis

The positioning error of the z-axis,  $\Delta z_{\text{pos}}$ , is less than 10  $\mu\text{in}$  [1].

### Uncertainty of the z-axis reference location

Recalling the results of the treatment of **Fixture Calibration**, we can assign the following uncertainties:  $\Delta\theta=0.001$  degree,  $\Delta r_{\text{ball}}=15$   $\mu\text{in}$ ,  $\Delta(\Delta Y_{AB})=14$   $\mu\text{in}$ ,  $\Delta r_{\text{FED}}=12$   $\mu\text{in}$  and  $\Delta d=0.0004$  in resulting in an estimated  $\Delta H=0.00045$  in (the error in d is grossly dominant). Then with  $\Delta z_{\text{ball}}=10$   $\mu\text{in}$ ,  $\Delta h_{\text{gage}}=20$   $\mu\text{in}$  and  $\Delta z_{\text{part}}=0.0015$  in we get  $\Delta z_{\text{ref}}\approx 0.002$  in.

### Variation of artifact thickness

This parameter deserves mention primarily to point out that, although the part-to-part variation is large,  $\pm 0.0015$  in (standard deviation) and so can through the motion control program affect the z locations at which data taking begins and ends, it does not enter into the calculation of the coordinate system in which the raw data are expressed.

### Total error in z

The uncertainty in the z axis reference location clearly dominates, giving  $\Delta z_{\text{total}} \approx 0.002$  in.

## Summary

The error in r will be by far the predominant contributor to uncertainty in the derived geometric dimensioning and tolerancing parameters (size, form, location and orientation) for the current artifact, which consists of cylinders whose axes are essentially parallel to the CMM spindle axis. The errors in z and  $\theta$ , while much larger, will influence these parameters relatively little. This will not necessarily be the case for other feature geometries and/or fixturing arrangements.

The uncertainty in the reference location is in all cases the largest single contributor to the uncertainty in any axis, so it is worthwhile to reduce this error term as much as possible. In general, the largest benefit will derive from a reduction in the z-axis reference uncertainty. It seems likely that all three linear axis references could be located more precisely by using a high quality cube, mounted with its faces parallel with the CMM planes of motion. The x and y references can be obtained by simply nulling the (properly oriented) indicator against the appropriate face of the cube. This should at least halve the  $\Delta r_{\text{ref}}$  term. The z reference is a little more difficult the deal with since the indicator cannot be lowered against the top of the cube. (The indicator is already fully deflected in the free state.) It should be possible to null the indicator against a vertical face of the cube, then sweep the cube in z while recording the indicator deflection. A plot of indicator reading vs. z will have a straight segment of almost constant

deflection and a curved segment corresponding to contact of the probe ball with the edge of the cube. These segments can be extrapolated to a repeatable reference location. The achievable precision is uncertain but is certainly closer to tens of  $\mu\text{in}$  than to the current figure of 0.002 in.

## VIII. REFERENCES

- [1] R. D. Pilkey and P. A. Klevgard, *Advanced Coordinate Measuring Machine at Sandia National Laboratories/California*, SAND93-8208, 1993, 32pp.
- [2] K. D. Summerhays, R. P. Henke, R. M. Cassou, J. M. Baldwin and C. W. Brown, 1995, *New Algorithms for the Evaluation of Discrete Point Measurement Data and for Sample Point Selection on Surfaces with Systematic Form Deviation*, Proceedings of the 10th Annual Meeting of the American Society for Precision Engineering, Austin, TX, 388-391.
- [3] J. M. Baldwin, R. P. Henke, K. D. Summerhays, R. M. Cassou and C. W. Brown, 1996, *Optimizing Discrete Point Sample Patterns and Measurement Data Analysis on Internal Cylindrical Surfaces with Systematic Form Deviations*, Proceedings of the International Manufacturing Engineering Conference, Storrs, CT, 447-449.
- [4] R. P. Henke, R. M. Cassou, K. D. Summerhays, J. M. Baldwin, and C. W. Brown, 1996, *Methodologies for the Evaluation of Systematic Form Deviations for Inside-Diameter Cylindrical Features and Their Relationship to Process Variables*, 11th Annual Meeting of the American Society for Precision Engineering, Monterey, CA, accepted for presentation.
- [5] anon., 1983, *Series 8200 CNC Programming Manual for Mill Applications*, Publication 8200-5.2.3, Allen-Bradley Co., Highland Heights, Ohio.
- [6] M. Majlak, *personal communication*, September 1995.

**Appendix A: Data Acquisition Program**



The following program, written in the HT BASIC language and running on a 386 PC under DOS was used to control the data acquisition. The program handshakes with the Allen Bradley motion control program *via* interrupts on the COM1 port. As shown in the Allen Bradley programs described in Appendix B, a control line on this port is toggled via coolant on/off commands which, in turn, drive a solid state relay. The listing is heavily commented and should be self-explanatory.

```

10 OPTION BASE 1                ! Filename: DITS_B
20 REAL A
30 DIM Filename$(40),Part_num$(8),Hole_str$(40),Hole$(10)[8]
40 INTEGER Counter,I,Sample,Sampsize(38),Num_holes,Hole
50 COM @Gpib,@Zygo,@Voltmeter,REAL Tzr(38,500,2)
60 Init_hpib                    ! Initialize the IEEE488 bus
70 Init_zygo                    ! Initialize the laser interferometer electronics
80 Init_voltmeter              ! Initialize the digital voltmeter
90 Init_com1                   ! Initialize the serial port
100 Num_holes=0
110 LINPUT "Enter Hole Numbers Separated By Commas:",Hole_str$
                                ! Get a list of hole numbers to be measured
120 Get_holes(Hole_str$,Hole$(*),Num_holes)
                                ! Parse the list
130 New_pass: INPUT "Enter Part Number:",Part_num$
                                ! Serial number of the current part
140 FOR Hole=1 TO Num_holes
150  Filename$="d:\dits\bw"&Hole$(Hole)&Part_num$&"_.000"
                                ! Build a filename based on hole & part numbers
160  OUTPUT CRT;Filename$      ! Display it
170  CREATE Filename$,1       ! Create a DOS ASCII file
180  ASSIGN @F TO Filename$   ! Open a path to it
190  FOR Counter=1 TO 38      ! Initialize z values to zero in the data array
200    FOR Sample=1 TO SIZE(Tzr,2)
210      Tzr(Counter,Sample,1)=0.
220    NEXT Sample
230  NEXT Counter
240  Counter=-1               ! So we know this is the start of data on this feature
250  REPEAT
260    IF (Counter<0) THEN    ! If the beginning of data acquisition on this feature
270      Counter=0           ! This won't happen again
280      STATUS 9,11;I       ! Read modem status to clear interrupt
290      ENABLE INTR 9;8     ! Interrupt if modem status changes
300      ON INTR 9 GOTO L10  ! Set branch destination for com1 interrupt
310 L:   GOTO L              ! Loop & wait
320 L10: GOSUB Read_xyz      ! Read x,y,z

```

```

330 ELSE ! These are the data acquisition passes
340 REPEAT ! We will do this 38 times
350 OFF INTR 9 ! Disable interrupt branch
360 Counter=Counter+1 ! Increment the scan counter
370 STATUS 9,11,I ! Read the modem status register; need to do this
! here to ensure we won't get stale data
380 ENABLE INTR 9;8 ! Interrupt if modem status changes
390 ON INTR 9,15 GOTO L11 ! Set branch destination for com1 interrupt
400 L1: GOTO L1 ! Loop & wait
410 L11: GOSUB Read_zr ! Read z & r
420 UNTIL (Counter=38) ! Test the loop counter
440 END IF
450 UNTIL (Counter=38)
460 Store_data(@F,Tzr(*),Sampsize(*)) ! Write the data file for this hole
470 ASSIGN @F TO * ! Close the file
480 NEXT Hole ! Repeat for all the holes on this part
490 GOTO New_pass ! Go back, get data for next part

500 Read_xyz: STATUS 9,11,I ! Read the modem status register to clear interrupt
510 Read_3d(X,Y,Z) ! Get the xyz location
520 OUTPUT @F USING "2(K,X),K";X,Y,Z
! Write it to the file
530 STATUS 9,11,I ! Read the modem status register
540 ON INTR 9,15 GOTO R1 ! Set the branch destination
550 ENABLE INTR 9;8 ! Re-enable com1 interrupt
560 L2:!
570 GOTO L2 ! Loop & wait
590 OFF INTR 9 ! Disable the interrupt branch
600 RETURN

610 Read_zr: STATUS 9,11,I ! Read the modem status register
620 Sample=0 ! Holds the number of samples in this pass
630 ON INTR 9 GOTO R2 ! Set the branch destination
640 ENABLE INTR 9;8 ! Enable the com1 interrupt
650 L3: ! Loop reading z and r
660 SEND 7;UNL LISTEN 23,24 ! Unlisten all devices, make laser & voltmeter
! listeners
670 TRIGGER 7 ! Trigger all listeners
680 DISABLE ! Disable interrupts while reading
690 OUTPUT @Zygo;"D1",END ! Latch the laser reading
700 ENTER @Zygo USING "-K";$$ ! Read the laser output
710 ENABLE ! Reenable the interrupt
720 A=NUM($$[1;1])+(256.*NUM($$[2;1]))+(65536.*NUM($$[3;1]))

```

```

730 A=A+(16777216*NUM(SS[4;1]))
740 A=A*(1.246046E-9)*100/(2.54)      ! Decode and scale the reading
750 Tzr(Counter,Sample+1,1)=A        ! Store the z value in the data array
760 ENTER @Voltmeter;Tzr(Counter,Sample+1,2)
                                       ! Read the voltmeter and store r in the data array
770 Sample=Sample+1                  ! increment the sample count
780 GOTO L3                           ! Loop until interrupt on com1
790 R2: STATUS 9,11;I                ! Read the modem status register
800                                   ! This code is needed to prevent the laser
810 SEND 7;UNL LISTEN 23,24          ! from getting locked up and from giving us
820 TRIGGER 7                         ! old latched data because we interrupted it
830 OUTPUT @Zygo;"D1",END            ! during a latch and read operation
840 ENTER @Zygo USING "-K";S$
850 ENTER @Voltmeter;A
860 FOR I=1 TO 10                    ! Needed to get last part of travel in z
870   Sample=Sample+1                ! Read a few more points while the z axis
880   SEND 7;UNL LISTEN 23,24        ! Decelerates
890   TRIGGER 7
900   OUTPUT @Zygo;"D1",END
910   ENTER @Zygo USING "-K";S$
920   A=NUM(SS[1;1])+(256.*NUM(SS[2;1]))+(65536.*NUM(SS[3;1]))
930   A=A+(16777216*NUM(SS[4;1]))
940   A=A*(1.246046E-9)*100/(2.54)
950   Tzr(Counter,Sample,1)=A
960   ENTER @Voltmeter;Tzr(Counter,Sample,2)
970 NEXT I
980 Sampsize(Counter)=Sample         ! Save the number of data points for this scan
990 OFF INTR 9                       ! Disable the interrupt branch
1000 RETURN

1010 END                             ! End of the main program

1020 SUB Init_com1
1030  OPTION BASE 1
1040  INTEGER I
1050  CONTROL 9,0;1                  ! Reset the serial port (device 9)
1060  STATUS 9,11;I                ! Read the modem status
                                       ! Needed to clear bit so an interrupt can happen
1070 SUBEND

1080 SUB Init_hpib
1090  OPTION BASE 1
1100  COM @Gpib,@Zygo,@Voltmeter,Tzr(*)

```

```

1110 ASSIGN @Gpib TO 7           ! Open a path to the IEEE488 bus
1120 ABORT 7                     ! Abort any operations in progress
1130 RESET 7                     ! Reset to power up status; assert IFC, clear
                                ! interrupts, set interface to be active controller
1140 CONTROL 7,0;1              ! Reset; DEC sent to IEEE488 card
1150 SUBEND

1160 SUB Init_voltmeter
1170 OPTION BASE 1
1180 COM @Gpib,@Zygo,@Voltmeter,Tzr(*)
1190 ASSIGN @Voltmeter TO 724    ! Open a path to the voltmeter
1200 OUTPUT @Voltmeter;"R2"     ! Set the resolution
1210 SUBEND

1220 SUB Init_zygo
1230 OPTION BASE 1
1240 COM @Gpib,@Zygo,@Voltmeter,Tzr(*)
1250 REAL A
1260 DIM Axes_status(3),Axesv(3),S$[4]
1270 ASSIGN @Gpib TO 7           ! Open a path to the IEEE488 bus
1280 ASSIGN @Zygo TO 723        ! Open a path to the laser electronics (device 23)

1290 ASSIGN @Volt to 724; FORMAT OFF
                                ! Open a path to the 3437A voltmeter (device 24)
1300 RESET 723                  ! Reset the laser to powerup state
1310 CLEAR 723                  ! Send SDC to the laser
1320 CONTROL 7,0;1              ! Reset IEEE488 control register
1330 OUTPUT @Zygo;CHRS(3)       ! Send <CTRL-C> to initialize laser
1340 WAIT 1
1350 OUTPUT @Zygo;"g1"          ! Set latch only mode
1360 WAIT 1
1370 OUTPUT @Zygo;"d4"          ! Binary mode output for laser
1380 WAIT 1
1390 OUTPUT @Zygo;"t3"          ! Send EOI on last character
1400 WAIT 1
1410 FOR I=1 TO 2
1420 B: SEND 7;UNL LISTEN 23,24 ! Unlisten all devices, make laser & voltmeter
                                ! listeners
1430 TRIGGER 7                   ! Trigger all listeners
1440 OUTPUT @Zygo;"D1",END       ! Latch the laser reading
1450 ENTER @Zygo USING "-K";S$   ! Read the laser output
1460 A=NUM(S$[1;1])+(256.*NUM(S$[2;1]))+(65536.*NUM(S$[3;1]))
1470 A=A+(16777216.*NUM(S$[4;1]))

```

```

1480  A=A*(1.246046E-9)*100/(2.54)  ! Decode and scale the reading
1490  NEXT I
1500  SUBEND

1510  SUB Read_3d(REAL X,Y,Z)        ! Reads a single xyz location
1520  COM @Gpib,@Zygo,@Voltmeter,Tzr(*)
1530  DIM S$(4)
1540  REAL A
1550  SEND 7;UNL LISTEN 23          ! Unlisten all devices, make laser a listener
1560  TRIGGER 7                    ! Trigger the laser
1570  OUTPUT @Zygo;"D1",END        ! Latch the laser z reading
1580  ENTER @Zygo USING "-K";S$    ! Read the laser output
1590  GOSUB Calc                   ! Decode and scale the reading
1600  Z=A                          ! Save it
1610  SEND 7;UNL LISTEN 23          ! Unlisten all devices, make laser a listener
1620  TRIGGER 7                    ! Trigger the laser
1630  OUTPUT @Zygo;"D2",END        ! Latch the laser y reading
1640  ENTER @Zygo USING "-K";S$    ! Read the laser output
1650  GOSUB Calc                   ! Decode and scale the reading
1660  Y=-A                          ! Save it - Y axis is inverted
1670  SEND 7;UNL LISTEN 23          ! Unlisten all devices, make laser a listener
1680  TRIGGER 7                    ! Trigger the laser
1690  OUTPUT @Zygo;"D3",END        ! Latch the laser x reading
1700  ENTER @Zygo USING "-K";S$    ! Read the laser output
1710  GOSUB Calc                   ! Decode and scale the reading
1720  X=A                          ! Save it
1730  SUBEXIT

1810  Calc: !
1820  A=NUM(S$(1;1))+(256.*NUM(S$(2;1)))+(65536.*NUM(S$(3;1)))
1830  A=A+(16777216.*NUM(S$(4;1)))
1840  A=A*(1.246046E-9)*100/(2.54)
1850  RETURN
1860  SUBEND

1870  SUB Store_data(@F,REAL Tzr(*),INTEGER Sampsize(*))
                                     ! This subprogram computes the angle values,
                                     ! writes theta, z, r records to the data file

1880  OPTION BASE 1
1890  DIM Ang$(18)
1900  INTEGER I,J,S
1910  REAL Theta
1920  Theta=0.
1930  Inc=.027*360.

```

```

1940 Theta=+Inc
1950 J=0
1960 FOR I=1 TO 37
1970   J=1
1980   S=Sampsize(I)
1990   Theta=Theta-Inc
2000   Ang$=VAL$(Theta)
2010   FOR J=1 TO S
2020     OUTPUT @F USING "2(K,X),K";Ang$,Tzr(I,J,1),Tzr(I,J,2)
2030   NEXT J
2040 NEXT I
2050 SUBEND

2060 SUB Get_holes(Hole_str$,Holes$(*),INTEGER Num_holes)
      ! This subprogram takes a comma-delimited string of hole numbers, returns a string array
      ! of the individual hole numbers and the hole count
2070 OPTION BASE 1
2080 INTEGER I,J
2090 DIM H$(40)
2100 H$=Hole_str$
2110 I=0
2120 WHILE (LEN(H$)>0)
2130   I=I+1
2140   J=POS(H$,",")
2150   IF (J=0) THEN
2160     Holes$(I)=H$
2170     H$=""
2180   ELSE
2190     Holes$(I)=H$[1,J-1]
2200     H$=H$[J+1]
2210   END IF
2220 END WHILE
2230 Num_holes=I
2240 SUBEND

```

While it is possible to enter motion control programs through the Allen Bradley control panel, it is more efficient to create them with a text editor and upload them through the serial port of the controller. The following listing, also in HT BASIC, provides a simple means to perform the upload.

```

10 OPTION BASE 1                                ! Program to upload motion control to the
                                                ! Allen Bradley serial port
20 INTEGER I

```

```

30 DIM A$[512],F$[50]
40 ASSIGN @C TO 9 ! Open the serial port
50 INPUT "ENTER Path\Filename",F$ ! Get the filename & path to upload
60 ASSIGN @F TO F$ ! Open the file
70 CONTROL 9,0;1 ! Reset the serial port
80 CONTROL 9,3;9600 ! 9600 baud
90 CONTROL 9,4;2
100 CONTROL 9,100;1 ! Enable XON\XOFF
110 ON ERROR GOTO L ! Detects EOF
130 FOR I=1 TO 2 ! Read & send until EOF
140 ENTER @F USING "K";A$
150 OUTPUT CRT;A$
160 OUTPUT @C USING "-,K";A$
170 WAIT 4
180 NEXT I
190 LOOP
200 ENTER @F USING "K";A$
210 OUTPUT CRT;A$
220 OUTPUT @C USING "-,K";A$
230 WAIT .6
240 END LOOP
250 L: OUTPUT @C;CHR$(4)
260 ASSIGN @F TO * ! Close the file
270 END

```

**Appendix B: Typical Motion Control Programs**



Following are listings of SCANMAIN, a typical measurement control main program for the Allen Bradley controller, and of POSINCYL and SCANCYL, the two macro programs that are called by any version of SCANMAIN to do the actual data acquisition. The listings show the program, in the Allen Bradley control language [5], and explanatory comments, which are delimited by /\*...\*/.

## SCANMAIN

SCANMAIN is the main motion control program. It positions the CMM relative to the artifact, then repetitively calls subprograms POSINCYL to position the probe in relation to each feature and SCANCYL to scan the surface of the feature.

```

% /*rewind stop character*/
(AP,PU=22.482824,PV=10.057850,PQ=-.1) /*assign parameters, PU=machine X location
of index hole, PV= machine Y location of index
hole, PQ=offset in X so probe will clear wall of
nominal hole (see notes)*/
(AP,PH=2.827415,PD=.1,PS=.2) /*assign parameters, PH=machine Z location of top
surface of part, PD=Z distance to move in hole
below surface of part when entering hole, PS=Z
clearance for traversing moves above part*/
(AP,P4=.5,P5=80) /*assign parameters, P4=delay time, P5=time to wait
to write scan to disk, seconds*/
M09 /*coolant off; used to toggle com1 interrupt, end
data taking*/
G90G70 /*absolute programming, move end points relative to
CAR zero position, inch mode*/
C0 /*move C axis to 0 position*/
M07 /*mist coolant on; used to toggle com1 interrupt;
start data taking*/
G04F,P4 /*dwell P4 seconds*/
M09 /*coolant off*/
(CM,POSINCYL,PX=2,PY=1.7,PU=PU,PV=PV,PQ=PQ,PH=PH,PD=PD,PS=PS) /*call macro
to position probe in hole to be scanned, PX=X
location of hole, PY=Y location of hole relative to
index hole*/
(CM,SCANCYL,PA=.5100) /*call macro to scan hole, PA= Z length of scan (see
notes)*/
G04F,P5 /*dwell P5 seconds to store data*/
G90 /*absolute programming*/
C0 /*move C axis to 0 position*/
M07 /*mist coolant on*/
G04F,P4 /*dwell P4 seconds*/

```

```

M09                                /*coolant off*/
(CM,POSINCYL,PX=1.7,PY=2,PU=PU,PV=PQ,PH=PH,PD=PD,PS=PS) /*call macro
to position for second hole*/
(CM,SCANCYL,PA=.5100)             /*call macro to scan second hole*/
G04F,P5                            /*dwell P5 seconds*/
G90                                /*absolute programming*/
C0                                 /*move C axis to 0 position*/
M07                                /*mist coolant on*/
G04F,P4                            /*dwell P4 seconds*/
M09                                /*coolant off*/
(CM,POSINCYL,PX=2,PY=2.3,PU=PU,PV=PQ,PH=PH,PD=PD,PS=PS) /*call macro
to position for third hole*/
(CM,SCANCYL,PA=.5100)             /*call macro to scan third hole*/
G04F,P5                            /*dwell P5 seconds*/
G90                                /*absolute programming*/
C0                                 /*move C axis to 0 position*/
M07                                /*mist coolant on*/
G04F,P4                            /*dwell P4 seconds*/
M09                                /*coolant off*/
(CM,POSINCYL,PX=2.3,PY=2,PU=PU,PV=PQ,PH=PH,PD=PD,PS=PS) /*call macro
to position for fourth hole*/
(CM,SCANCYL,PA=.5100)             /*call macro to scan fourth hole*/
G04F,P5                            /*dwell P5 seconds*/
G90                                /*absolute programming*/
C0                                 /*move C axis to 0 position*/
G01Z7                             /*retract quill to Z=7 inches*/
M30                                /*end of program, rewind tape*/

```

Notes:

- 1) Example main motion control program for data acquisition on four features.
- 2) This assumes quill axis will be positioned on feature axis and indicator is set up for proper size hole.
- 3) Z length of scan is computed as follows:
  - a. For a through hole,  $PA = \text{nominal depth} + 0.01 \text{ inch}$ .
  - b. For a blind hole,  $PA = \text{nominal depth} - (\text{ball radius} + \text{tolerance on depth} + 0.01 \text{ inch})$
- 4) Dwell length, in seconds, to store data is  $P5 = 130 * \text{hole depth in inches}$ .
- 5) See reference 5 for details of Allen Bradley programming language.

## POSINCYL

This subprogram is called by SCANMAIN, once per feature, and positions the CMM relative to the feature.

```
%                               /*rewind stop character*/
(DM,POSINCYL)                   /*define macro named POSINCYL*/
G01Z,(PH+PS)                     /*move in Z, linear interpolation, to top of part(PH)
                                + clearance(PS)*/
G01X,(PU+PX+PQ)                 /*move in X to index hole location + feature
                                location + offset to keep probe from surface of
                                hole*/
G01Y,(PV+PY)                   /*move in Y to hole location + feature location*/
G01Z,(PH-PD)                   /*move in Z, PD into hole from top of part*/
G01X,(PU+PX)                   /*move in X, to position probe against surface of
                                hole*/
G01Z,(PH)                       /*move in Z, to position probe center in top plane of
                                part*/
(EM)                             /*end macro*/
(EM)
T                               /*rewind*/
→
```

## SCANCYL

This subprogram is called by SCANMAIN, once per feature, and scans the feature.

```
%                               /*rewind stop character*/
(DM,SCANCYL)                   /*define macro to scan a full cylinder*/
(AP,P2=0,P3=19,P4=.5)         /*assign parameters, P2=scan counter, initialized to 0, P3= number
                                of bidirectional scans to be made, P4= dwell time*/
G90                             /*incremental programming, move destinations are relative to
                                current location*/
L1                              /*L-word for if-then destination*/
M07                             /*mist coolant on, toggle com1 interrupt to start taking data*/
G01Z,-PA                       /*linear interpolation, move in Z to scan depth*/
M09                             /*coolant off, toggle com1 interrupt to stop taking data*/
G04F,P4                       /*dwell P4 seconds*/
C-.02700                       /*rotate C axis 0.027 revolution*/
G04F,P4                       /*dwell P4 seconds*/
M07                             /*mist coolant on*/
G01Z,PA                       /*scan in Z back to top of part*/
```

```
M09                /*coolant off*/
G04F,P4           /*dwell P4 seconds*/
C-.02700         /*rotate C axis 0.027 revolution*/
(AP,P2=P2+1)     /*increment P2*/
(IFT,P2,LT,P3,L1) /*if P2<P3 goto L1 and scan again*/
(EM)            /*end macro*/
(EM)
T                /*rewind*/
-
```

**Appendix C: Machine Drawing of Cylinder Artifact**

$\text{⌀ } \text{⌀} .010 \text{ M A S M}$   
 Applies to Holes 3-46

2X  $\text{⌀} 0.375 \pm 0.005$

$\text{⌀} .005 \text{ M A}$

-S-

$\text{⊥ } \text{⌀} 0.500 \pm 0.005 \text{ TO } \nabla$   
 SHOWN ON BOTH SIDES

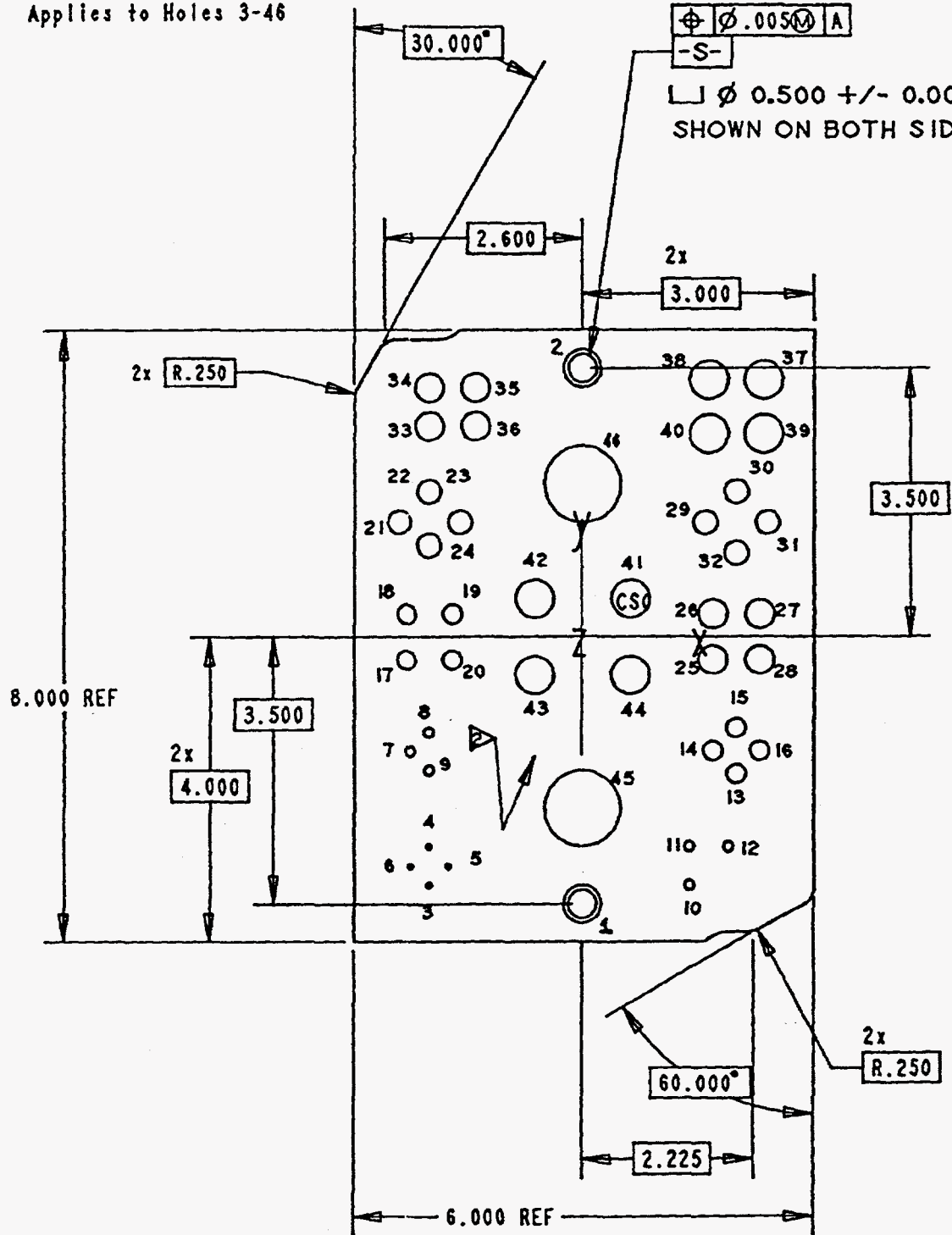


Figure 12. Cylinder artifact; top view.

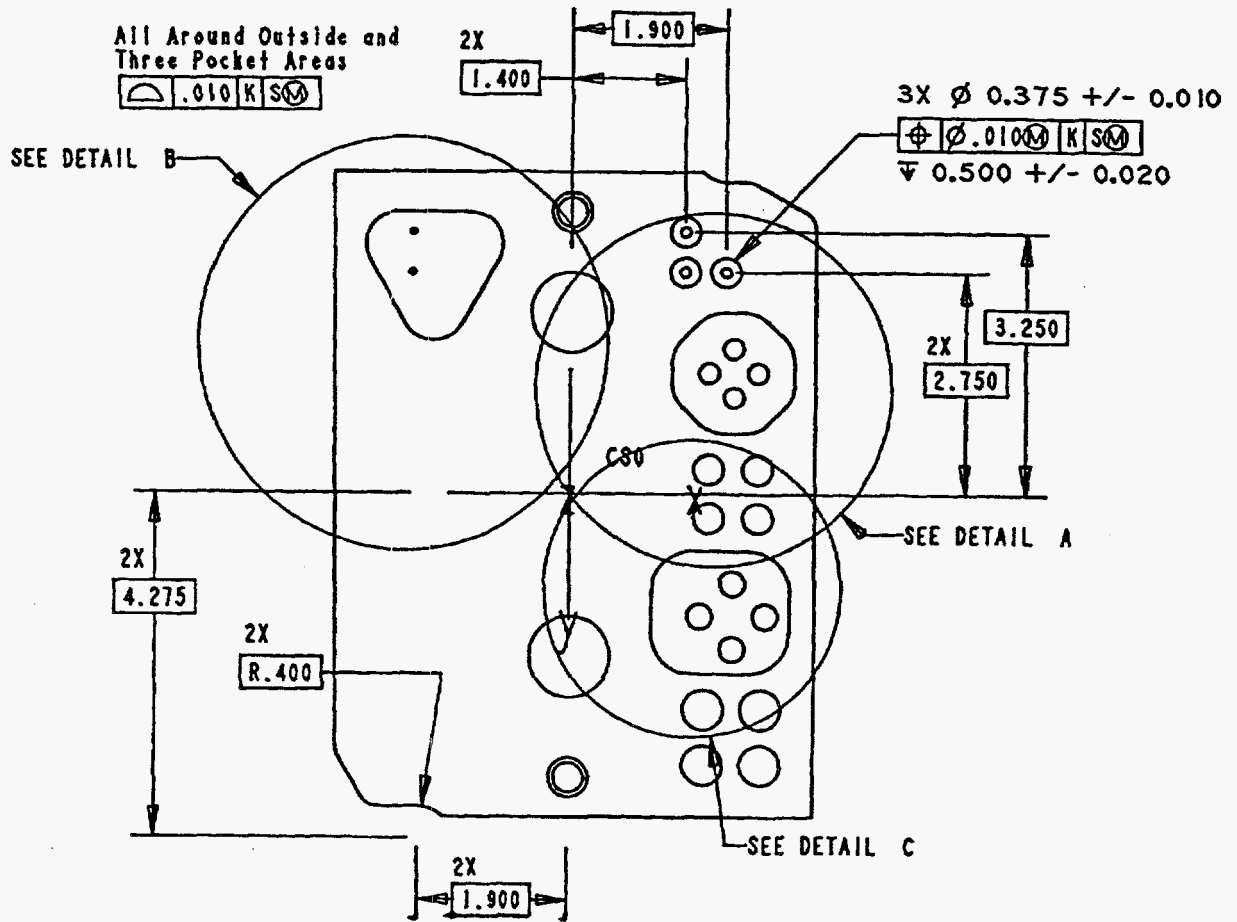


Figure 13. Cylinder artifact; bottom view.

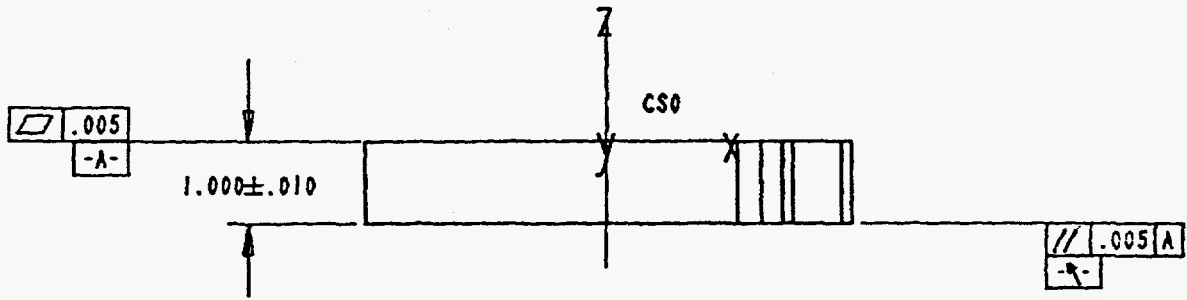
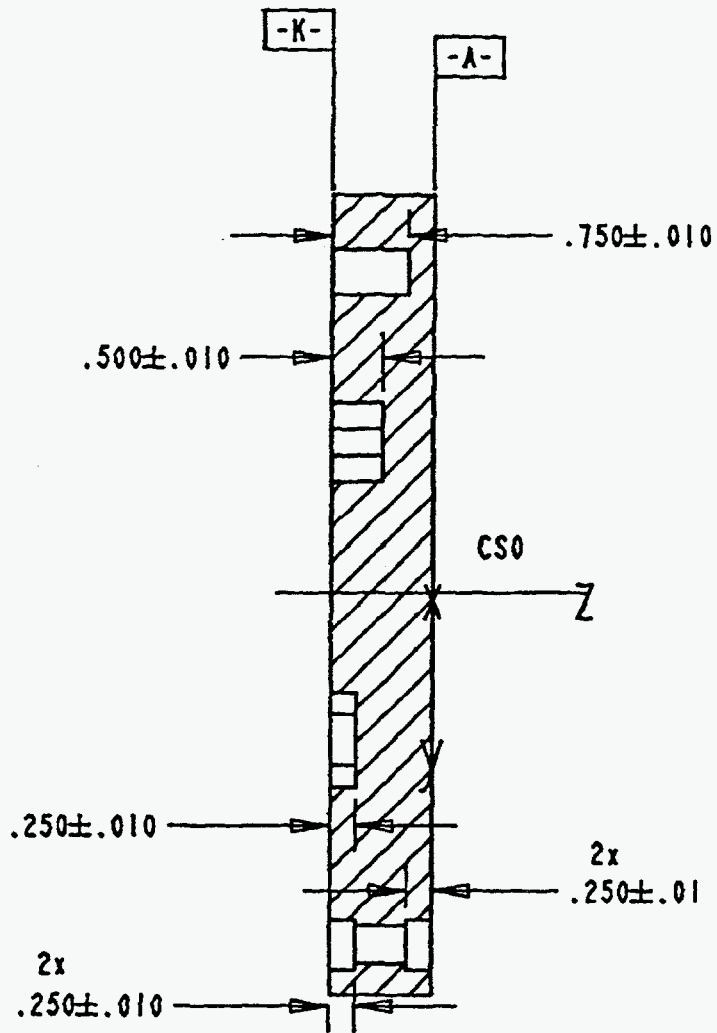


Figure 14. Cylinder artifact; side view.



SECTION POCKET DEPTHS-POCKET DEPTHS

Figure 15. Cylinder artifact; section view.



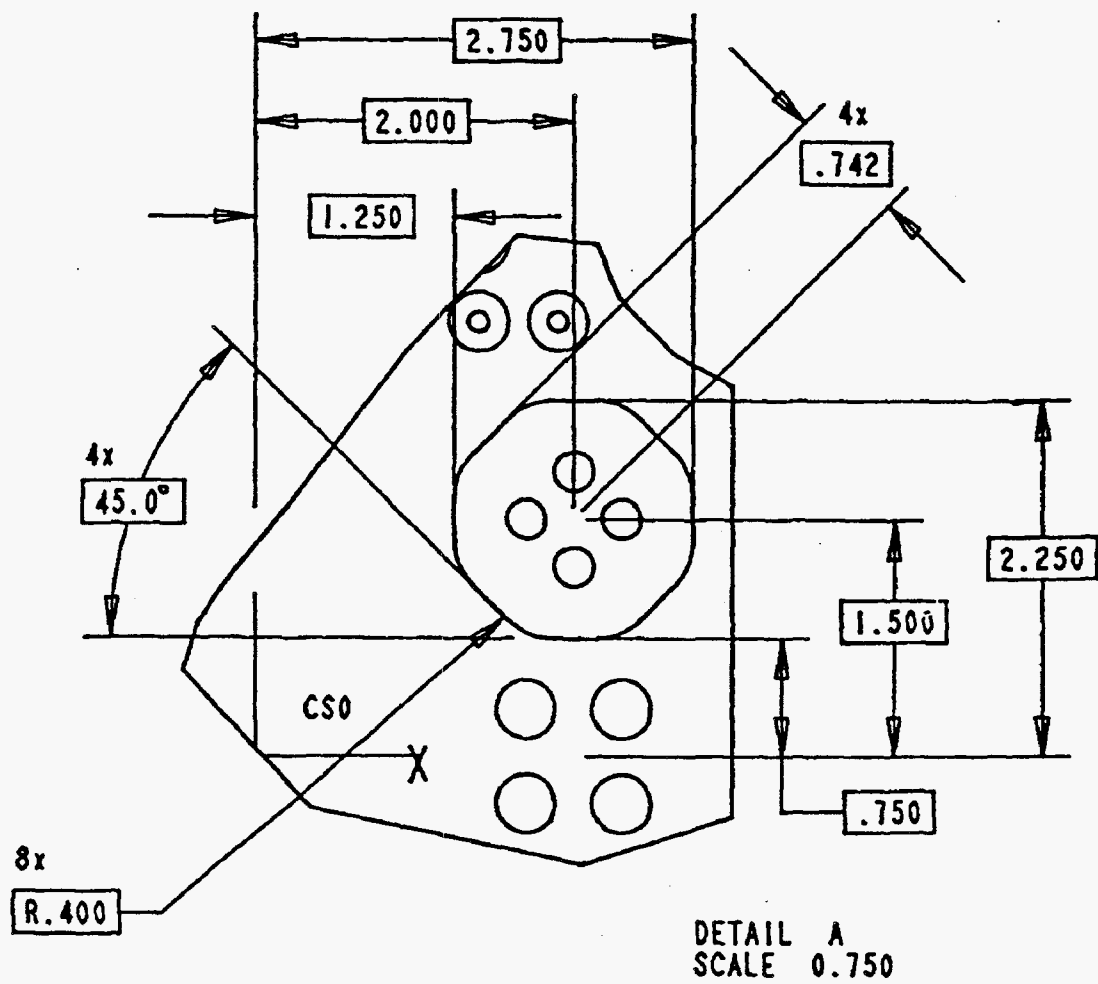
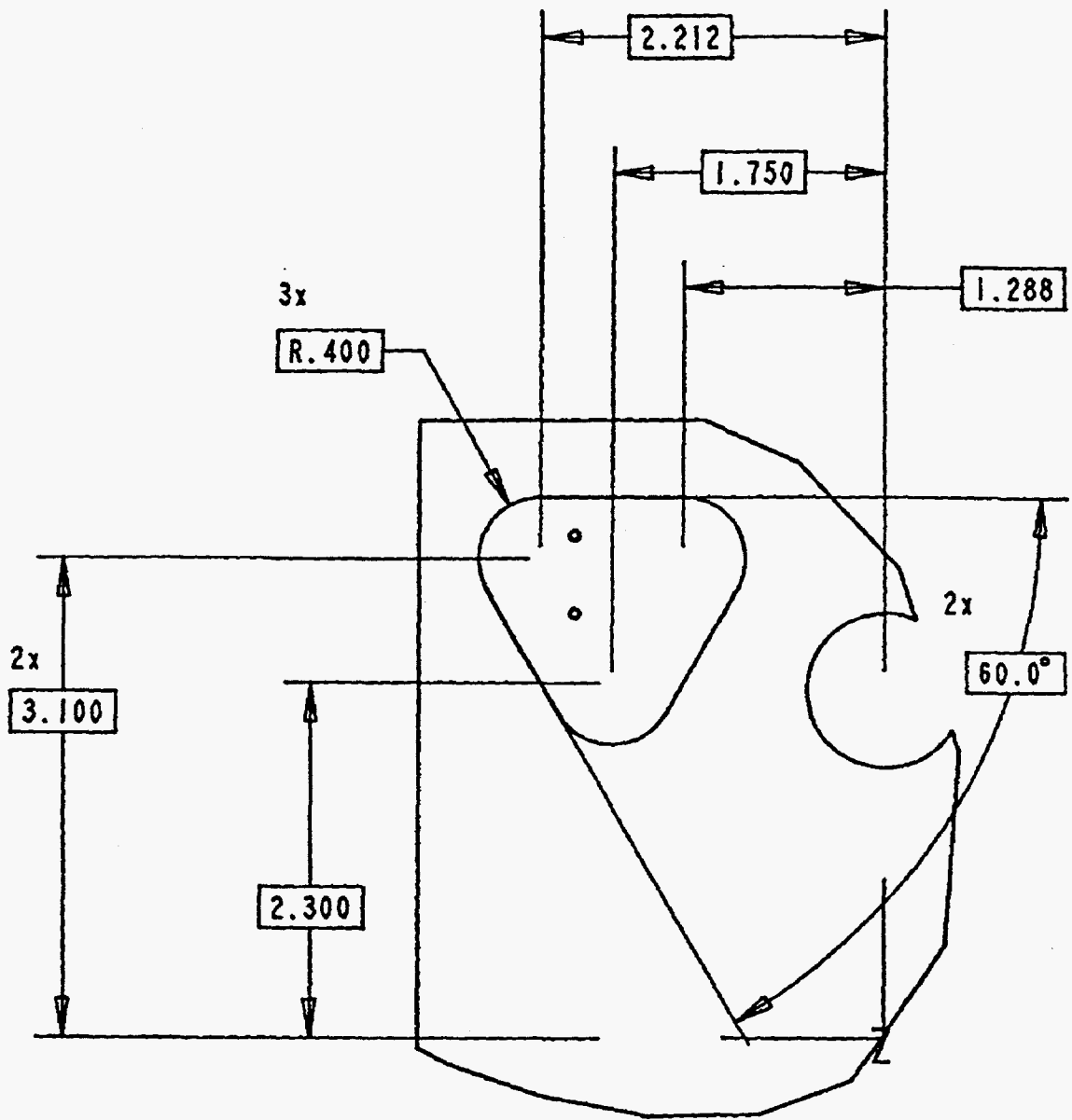
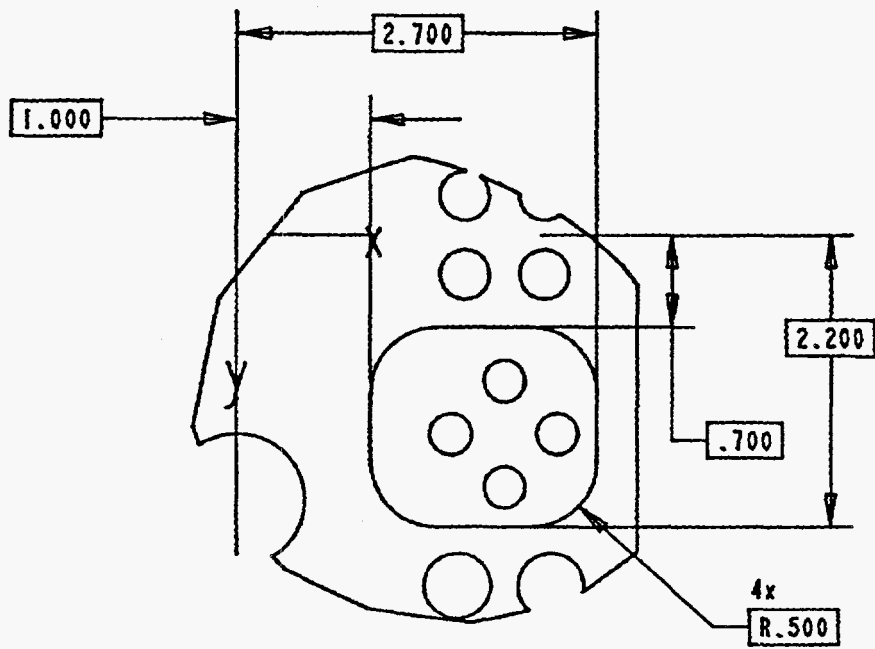


Figure 16. Cylinder artifact; detail A.



DETAIL B  
 SCALE 0.750

Figure 17. Cylinder artifact; detail B.



DETAIL C  
SCALE 0.750

Figure 18. Cylinder artifact; detail C.

**Table C-1. List of Full Cylindrical Features on the Artifact.**

Hole #*	X Dim.	Y Dim.	Dia. ±0.005	Full Dia. Depth ±0.020	Blind/ Through/ Counter	Mfg. Process**
1	0.000	-3.500	0.375	0.500	T	C/D
1A	0.000	-3.500	0.500	0.250	C	C/D/M
1B	0.000	-3.500	0.500	0.250	C	C/D/M
2	0.000	3.500	0.375	0.500	T	C/D
2A	0.000	3.500	0.500	0.250	C	C/D/M
2B	0.000	3.500	0.500	0.250	C	C/D/M
3	-2.000	-3.250	0.0625	0.250	T	C/D
4	-2.000	-2.750	0.0625	0.250	T	C/D/R
5	-1.750	-3.000	0.0625	0.1875	B	C/D
6	-2.250	-3.000	0.0625	0.1875	B	C/D/R
7	-2.250	-1.500	0.125	0.375	B	C/D
8	-2.000	-1.250	0.125	0.375	B	C/D/R
9	-2.000	-1.750	0.125	0.375	B	C/D/B/R
10	1.400	-3.250	0.125	0.500	T	C/D
11	1.400	-2.750	0.125	0.500	T	C/D/R
12	1.900	-2.750	0.125	0.500	T	C/D/B/R
13	2.000	-1.800	0.250	0.500	T	C/D
14	1.700	-1.500	0.250	0.500	T	C/D/R
15	2.000	-1.200	0.250	0.500	T	C/D/B/R
16	2.300	-1.500	0.250	0.500	T	C/D/P
17	-2.300	-0.300	0.250	0.750	B	C/D
18	-2.300	0.300	0.250	0.750	B	C/D/R
19	-1.700	0.300	0.250	0.750	B	C/D/B/R

Table C-1(cont). List of Full Cylindrical Features on the Artifact.

Hole #*	X Dim.	Y Dim.	Dia. ±0.005	Full Dia. Depth ±0.020	Blind/ Through/ Counter	Mfg. Process**
20	-1.700	-0.300	0.250	0.750	B	C/D/P
21	-2.400	1.500	0.3125	0.700	B	C/D
22	-2.000	1.900	0.3125	0.700	B	C/D/R
23	-1.600	1.500	0.3125	0.700	B	C/D/B/R
24	-2.000	1.200	0.3125	0.700	B	C/D/P
25	1.700	-0.300	0.375	1.000	T	C/D
26	1.700	0.300	0.375	1.000	T	C/D/R
27	2.300	0.300	0.375	1.000	T	C/D/B/R
28	2.300	-0.300	0.375	1.000	T	C/D/P
29	1.600	1.500	0.3125	0.750	T	C/D
30	2.000	1.900	0.3125	0.750	T	C/D/R
31	2.400	1.500	0.3125	0.750	T	C/D/B/R
32	2.000	1.100	0.3125	0.750	T	C/D/P
33	-2.000	2.750	0.375	0.700	B	C/D
34	-2.000	3.250	0.375	0.700	B	C/D/R
35	-1.400	3.250	0.375	0.700	B	C/D/B/R
36	-1.400	2.750	0.375	0.700	B	C/D/P
37	2.350	3.350	0.500	1.000	T	C/D
38	1.650	3.350	0.500	1.000	T	C/D/R
39	2.350	2.650	0.500	1.000	T	C/D/B/R
40	1.650	2.650	0.500	1.000	T	C/D/P
41	0.625	0.500	0.500	0.650	B	C/D
42	-0.625	0.500	0.500	0.650	B	C/D/R

**Table C-1(cont). List of Full Cylindrical Features on the Artifact.**

<b>Hole #*</b>	<b>X Dim.</b>	<b>Y Dim.</b>	<b>Dia. ±0.005</b>	<b>Full Dia. Depth ±0.020</b>	<b>Blind/ Through/ Counter</b>	<b>Mfg. Process**</b>
43	-0.625	-0.500	0.500	0.650	B	C/D/B/R
44	0.625	-0.500	0.500	0.650	B	C/D/P
45	0.000	-2.250	1.000	1.000	T	C/D
46	0.000	2.000	1.000	1.000	T	C/D/R

\*Refer to hole numbers on drawing.

\*\*C=center drill, D=drill, R=ream, B=bore, P=plunge end mill, M=mill

UNLIMITED RELEASE

INITIAL DISTRIBUTION

Ronald M. Cassou  
Harney Science Center  
University of San Francisco  
2130 Fulton Street  
San Francisco, California 94117-1080

Kim D. Summerhays  
Harney Science Center, Room 409  
University of San Francisco  
2130 Fulton Street  
San Francisco, California 94117-1080 (3)

Richard P. Henke  
MicroVu  
7909 Conde Lane  
Windsor, California 95492

C. W. Brown  
Allied Signal FM&T  
2000 E. 95th St.  
PO BOX 419159,D/458,2B27  
Kansas City, Missouri 64141-3548

MS9001	T. O. Hunter, 8000	
	Attn: MS9005	J. B. Wright, 2200
	MS9004	M. E. John, 8100
	MS9054	W. J. McLean, 8300
	MS9007	R. C. Wayne, 8400
	MS9002	P. N. Smith, 8500
	MS9405	T. M. Dyer, 8700
	MS9141	P. Brewer, 8800
	MS9003	D. L. Crawford, 8900
MS9133	J. M. Baldwin, 8220 (20)	
MS9133	K. A. Hontz, 8220	
MS9133	R. D. Pilkey, 8220 (10)	
MS9420	L. A. West, 8200	
	Attn: MS9430	L. N. Tallerico, 8204
	MS9404	B. E. Affeldt, 8210
	MS9405	M. H. Rogers, 8220
	MS9405	J. M. Hruby, 8230

	MS9430	A. J. West, 8240
	MS9133	J. A. Fordham, 8240-1
	MS9409	R. H. Stulen, 8250
	MS9107	V. C. Barr, 8250-1
MS9405	Manager, 8220	
MS0953	W.E. Alzheimer, 1500	
MS0665	L. J. Azevedo, 1541	
MS9021	Technical Communications Department, 8535, for OSTI (10)	
MS9021	Technical Communications Department, 8535/Technical Library, MS0899, 13414	
MS0899	Technical Library (4)	
MS9018	Central Technical Files, 8523-2 (3)	